Calculated Physicochemical Properties of Glycerol-derived Solvents to Drive Plastic Waste Recycling

Ademola Soyemi [a] *and Tibor Szilvási* [a]*

[a] Department of Chemical and Biological Engineering, University of Alabama, Tuscaloosa, Alabama 35487, United States.

* Email: tibor.szilvasi@ua.edu

ABSTRACT

Plastic waste has become a major environmental crisis, with majority of plastic being produced ending up in open landfills and water ways every year. Solvent-based recycling approaches offer an effective means of recovering high-quality plastic material from waste by use of a solvent to selectively dissolve the plastic waste and recover specific polymers. In this work, we report on the properties of 9587 potential glycerol-based solvents that can be synthesized from biomass-derived glycerol. We predict the density and dipole moment using quantum mechanical calculations, while the LogS, LogP, and the melting point are predicted using machine learning that outperforms other prediction methods such as Hansen Solubility Parameters in Practice (HSPiP). Additionally, we analyze the ability of the solvents to dissolve common plastic materials (polyethylene (PE), polyethylene terephthalate (PET), polyether sulfone (PES), polypropylene (PP), polystyrene (PS),

and polyvinyl chloride (PVC)) based on a comparison of their Hansen Solubility Parameters (HSPs). Our results show that functionalization of glycerol can significantly alter its properties, and based on the HSPs and melting point, we recommend selective solvents for PE, PET, and PVC, while for PES, PP and PS, we suggest using a combination of solvents in a solvent/antisolvent setup for solvent-based plastic waste recycling. Finally, based on stricter solvent selection criteria we also propose a strategy that may help reduce costs of sorting waste plastic whereby the waste feedstock is first separated into polar and non-polar fractions.

1. INTRODUCTION

Plastics have transformed society, allowing us to make a variety of household and industrial materials on which modern society is now highly dependent. Since industrial scale plastic production started in the 1950s, plastic production has been steadily rising reaching approximately 400 million tons in 2021 and is estimated to surpass 1.1 billion tons by 2050 as manufacturing becomes more efficient and the feedstocks cheaper.[1, 2] However, the plastic waste associated with plastic production and use is mostly non-biodegradable and is typically mismanaged. A recent report shows that only around 14% of plastics are recycled and around 85% end up in landfills or are incinerated, while the rest end up in water bodies.[3] These waste plastics that end up in landfills and water bodies ultimately mechanically degrade and create microplastics that harm marine life and as a consequence human life since microplastics can end up in food and drinking water.[4] Because of this, many countries have started implementing policies to incentivize plastics recycling and cleanup initiatives, however recycling rates vary wildly with the US recycling 10%, the EU 31%, and most of the developing world not recycling at measurable scale.[5] Despite the problems posed by plastic waste, plastic recycling remains challenging for a number of reasons including: (1) varying compositions of plastics, (2) high capital investment required, and (3)

difficulty of sorting different plastic materials and contaminants.[6] These limitations mainly apply to the most common method of plastic waste recycling, known as mechanical recycling which involves breaking down of sorted and cleaned plastic waste into smaller flakes which are then processed into new material. In addition to the aforementioned limitations, the majority of new plastic material produced via mechanical recycling is 'down-cycled' which means that the new material is of less quality than the virgin plastic material.[6]

To overcome limitations associated with mechanical recycling, chemical recycling which either involves a solvent-based[7, 8] or reaction-based[9, 10] approach offers a viable alternate for 'recycling' waste plastic that can be competitive with virgin plastic materials.[7, 11] Solvent-based recycling involves recovery of plastic material without chemically altering the structure of the material and follows a simple workflow. First the target plastic is selectively dissolved in the solvent at a specific temperature. This is followed by filtration of the resulting mixture to recover the liquid phase which contains the solvated plastic. Finally, the dissolved polymer is recovered by either the addition of an antisolvent (i.e. solvent in which plastic is insoluble) or by temperature swing (i.e. change in temperature causing solvated plastic to precipitate out of solution).[12, 13]

The key challenge of the solvent-based approach is the selection of an appropriate solvent(s), which ideally selectively dissolves only the target polymer while keeping out unwanted materials such as additives and plasticizers. The solvent-based approach, however, is not a new idea as dissolution and separation of polymeric materials has been demonstrated experimentally and disclosed in patents from various companies since the 1930s.[6, 7] For example, Sändig demonstrated the dissolution and separation of condensation products, mostly polyesters, using ethyl alcohol as a solvent in 1936.[14] In another patent received by the Standard Oil Development Company in 1945, researchers developed a method for the separation of polyesters using paraffin mineral oils as a

solvent.[15] These initial studies demonstrated the use of solvents in purification of polymerization products and gave way to the eventual use of solvents for dissolution of plastic materials beginning in the 1970s. Wainer et al., demonstrated a method for the dissolution of polyvinyl chloride (PVC),[16] while Mizumoto et al., showed a general method to selectively separate an individual polymer from a mixture of polymers.[17] Seymour and Stahl demonstrated the dissolution and separation of polyethylene (PE), PVC, polystyrene (PS), polyvinyl acetate (PVAC), and polymethyl methacrylate (PMMA) using a series of common solvents such as methanol, petroleum ether, and toluene based on their solubility parameters.[18]

As a field, solvent-based plastic recycling has been industry-driven with developments mainly being disclosed in the form of patents. However, nowadays solvent-based recycling is also gaining interest in scientific literature.[19-25] For instance, Achilias and co-authors demonstrated high polymer recovery rates (>90%) in several studies, for the recycling of various polymers obtained from waste electric equipment,[21] and packaging materials,[19, 20] using solvents such as toluene, xylene, n-hexane, acetone, chloroform, and methanol. Kartalis et al., also reported the selective dissolution and recovery of polycaprolactam and poly(hexamethylene adipamide) from polymer mixtures using dimethyl sulfide (DMSO), and formic acid as solvents for each polymer.[22] Walker, et al.,[12] demonstrated a computationally-guided strategy, called solvent-targeted recovery and precipitation (STRAP), to deconstruct multi-layer plastic materials (three or more layers) into their component resins (polyethylene (PE), polyethylene terephthalate (PET), and ethylene vinyl alcohol (EVOH)) via a series of solvent washes. In another study by Sánchez-Rivera, et al., the STRAP process was further analyzed by comparing different polymer precipitation techniques – precipitation by antisolvent addition (STRAP-A), and precipitation by decreasing the solvent temperature (STRAP-B).[26] In addition, the authors also demonstrated that the STRAP process is

applicable to more complex multilayer systems by use of antisolvent for precipitation of certain resins and reduction of temperature for precipitation of other resins in a process called STRAP-C.[26] In these studies, the solvents used to dissolve the studied plastics included common solvents such as toluene, DMSO, and acetone. These solvents pose potential industrial safety hazards as well as harm to the environment, human, and wildlife due to their volatility and toxicity which may limit the applicability of these solvents to large-scale industrial operation. These limitations necessitate the use of safe, environmentally friendly solvents for large-scale solvent-based plastic recycling operations. However, only few studies are present in literature which report dissolution of plastics using 'green' solvents produced from sustainable sources.[27-31] For example, Hattori et al., demonstrated the dissolution of polystyrene (PS) in p-cymene and similar compounds present in tree leaf oils. In their study, they achieved a solubility of 212.0 ± 0.2 (g PS/100g solvent) and a recovery rate of 96.3 ± 0.4 % using p-cymene. Due to heterogeneous nature of plastic waste, however, the unavailability of a database of green solvents with a wide range of properties represents a major challenge to the rapid development of solvent-based plastic recycling technology. Design of such solvents must follow certain design rules to be viable industrially including: (1) low viscosity, (2) low density, (3) low vapor pressure, (5) non-toxic, and (6) cheap to produce in addition to favorable solubility of different plastic materials.

In this work, we report a library of solvents which were designed using glycerol as a platform molecule that can be obtained from renewable biomass at affordable cost.[32-34] Previous studies have shown that through a simple synthesis procedure using epichlorohydrin, glycerol can be functionalized to produce solvents with a wide array of physical properties depending on the functional group.[32-41] Additionally, synthesis of glycerol derivatives has been shown to exhibit at least seven advantages within the twelve rules of green chemistry, such as waste prevention, atom

economy, solvent safety, energy efficiency, renewable feedstock, reduced derivatization, and real-time analysis.[33] These compounds have been shown to have low viscosities compared to glycerol, and are compatible with common organic solvents.[38, 39] Furthermore, they have also been shown to be non-toxic.[42] Here, we report four classes of glycerol-derived solvents, namely glycerol-derived alcohols (GDAs), glycerol-derived ketones (GDKs), glycerol-derived ethers (GDEs), and glycerol-derived deoxygenates (GDDs), along with their thermophysical properties such as density, water solubility (LogS), lipophilicity (LogP), melting point as well as their Hansen Solubility Parameters (HSPs). We have chosen these classes of glycerol-derivatives in order to obtain a large library of potential environmentally friendly alternatives to conventional solvents for plastic recycling applications. Furthermore, as demonstrated in previous works,[37, 40, 41] these solvents can be efficiently produced using a variety of polar, non-polar, and aromatic 'R' groups shown in Scheme 1. By changing the functional groups in different ether sites, properties such as density, dipole moment, water solubility, hydrophobicity, and so on, can be altered to meet requirements for different applications. For example, Qian et al., showed that the density of glycerol-derivates functionalized with alkyl groups was lower than that of glycerol, while the density of glycerol-derivatives functionalized with trifluoromethyl groups had a higher density regardless of arrangement (i.e. symmetric vs asymmetric).[33] In addition, they have also shown that depending on the functional group and arrangement, the miscibility in various polar and non-polar solvents can be tuned.[32, 33, 36] These studies, however, have been limited to alkyl/alkyl ether, and trifluoromethyl groups and consequently we extend these studies by considering a wider array of functionalization with groups such as cyclics (cyclopropyl, cyclobutyl, and cyclohexyl), amine, cyano, phenyl-nitrile, biphenyl-nitrile, halides, and methyl halides. In addition, most work on glycerol derivates has been done with GDAs, GDKs, and GDEs, therefore, we have also

considered deoxygenates of glycerol (GDDs in Scheme 1) where the central ether site has been replaced with a halide, cyano, or amine group or saturated with a hydrogen atom. This enables the study of a variety solvents with a wide range of physical properties. Accordingly, we catalogue 9587 potential solvents and their physicochemical properties. We have also evaluated the solvents as candidates for dissolution of polar plastics such as polyvinyl chloride (PVC), polyethylene teraphthalate (PET), polyether sulfone (PES), and non-polar plastics such as polyethylene (PE), polypropylene (PP), and polystyrene (PS) using HSPs. Thus, this work can serve as a reference for future computational and experimental studies of glycerol-derivatives for solvent-based plastic recycling.

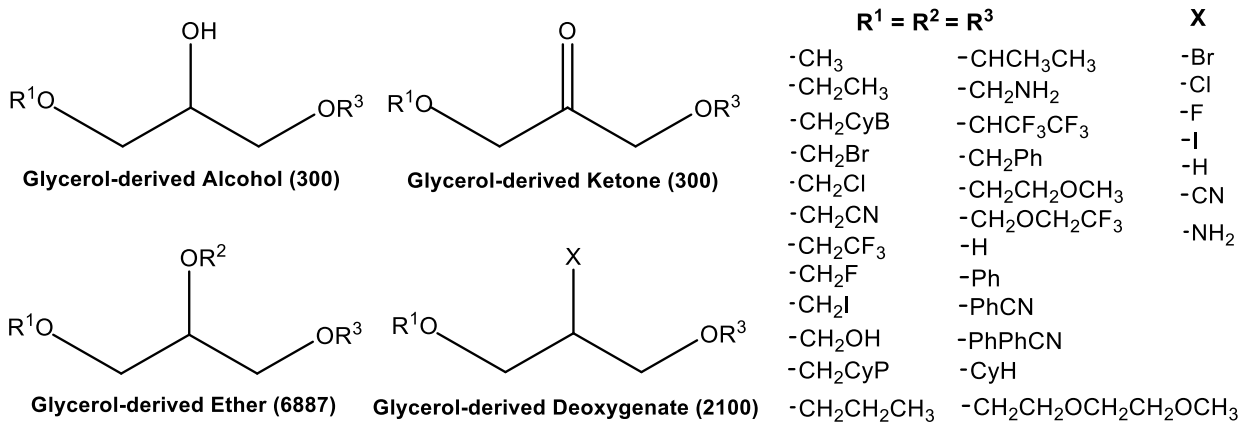

Scheme 1. Basic structure for a) glycerol-derived alcohols (GDA), b) glycerol-derived ketones (GDKs), c) glycerol-derived ethers (GDEs), and d) glycerol-derived deoxygenates (GDDs). Below each structure is the number of compounds in that category with the entire dataset totaling 9587 molecules. Note that CyB, CyP, and CyH represent cyclobutane, cyclopropane, and cyclohexane, respectively.

From our work, we show that the properties of glycerol derivatives are highly tunable depending on the functional groups attached. We also show glycerol derivates outperform glycerol in ability to dissolve polar (PET, PES, PVC) and non-polar plastic materials (PE, PP, PS). Additionally, we

provide potential glycerol-derived solvents which are predicted to carry out selective plastic dissolution based on their melting point and HSPs.

2. COMPUTATIONAL METHODS

To build a library of glycerol-based solvents, we have defined four subcategories with glycerol as the backbone, namely i) glycerol-derived alcohols (GDAs), ii) glycerol-derived ketones (GDKs), iii) glycerol-derived ethers (GDEs), and iv) glycerol-derived deoxygenates (GDDs) shown in Scheme 1. Scheme 1 also shows a list of functional groups used to create a variety of potential solvent candidates. Based on these functional groups, we combinatorically created a SMILES-based[43] list of 9587 solvent candidates (see Scheme 1 for population of each subcategory). The SMILES[43] representation of each molecule was canonicalized and converted into XYZ coordinates using OpenBabel (version 2.4.0)[44] and used for further calculation of physical properties as detailed in the sections below.

2.1. Calculation of Solvent Physical Properties

2.1.1. Dipole Moment Prediction

The dipole moments of the solvent compounds in the gas phase were calculated using a combined semi-empirical and first principles quantum chemical approach. An initial search of stable conformations of each solvent molecule was performed using the GFN-FF force field[45] in CREST[46] as implemented in the xTB program.[47] This was followed by a geometry optimization of each conformation using the GFN2-xTB semi-empirical method,[48] also implemented in the xTB program, which has been shown to produce good geometries and dipole moments.[49] From this, the ten most stable conformations were selected for further calculations. The dipole moment of the ten most stable conformations were then computed at Density Functional Theory (DFT) level using the GAUSSIAN 16 program[50] by performing single point energy calculations with the B3LYP

functional[51] and the D3 empirical dispersion scheme,[52] together with the def2-SVP basis set.[53] Finally, the average dipole moment of each solvent molecule was then computed as the Boltzmann-average of the studied ten most stable conformations.

2.1.2. Density Prediction

The thermophysical properties of the solvent molecules were calculated using the COSMOtherm software package (BIOVIA COSMOtherm, Release 2020)[54] which has been shown to be a practical method of predicting physical properties of similar solvent molecules.[36, 41] The density was obtained for each solvent molecule over a temperature range of 20 °C to 80 °C. The required COSMO files needed for property calculation in COSMOtherm were generated based on DFT calculations performed using the GAUSSIAN 16 program. The most stable conformation of each solvent molecule (based on GFN2-xTB geometry optimization) was further optimized using the BP86 functional[55, 56] and the TZVP basis set[57] except for iodine-containing compounds since the TZVP basis set was not parameterized with for iodine atoms. Thus, optimized structures for iodine-containing compounds were obtained using the def2-TZVP basis set[53] on the iodine atom, and the TZVP basis set for all other atoms. Single point energy calculations were then performed with the BP86 functional together with the TZVP basis set and the COSMO-RS solvation[58, 59] model to obtain the necessary COSMO files following previous studies that had predicted physical properties of liquid-phase compounds.[35, 60, 61] Similarly for iodine-containing molecules, single point energy calculations were carried out using the BP86 functional and the def2-TZVP basis set defined for the iodine atom (TZVP basis set defined for all other atoms) together with the COSMO-RS solvation model. Finally, we performed COSMO calculations in the COSMOtherm software package (BIOVIA COSMOtherm, Release 2020) at the TZVP level.

2.1.3. Calculation of Hansen Solubility Parameters (HSPs)

We assessed the solubility of polar and non-polar plastic materials, namely polyvinyl chloride (PVC), polyethylene terephthalate (PET), polyether sulfone (PES), polyethylene (PE), polypropylene (PP), and polystyrene (PS), which are commonly found in plastic waste streams,[62] using the HSPs of the solvent molecules and polymers. HSPs are empirical parameters for solvents which are used as a measure to identify solvents that are capable of dissolving target polymer materials.[63-65] Each compound (solvent or polymer) are characterized by three HSPs that describe the strength of dispersion interactions (δ_D), polar or dipole-dipole interactions (δ_P), and hydrogen-bonding interactions (δ_H).[63, 64] These parameters define the coordinates of each compound within the Hansen space. Each polymer has an additional parameter known as the radius parameter (R_0), determined by experimentally quantifying the solubility of the polymer in various solvent systems,[64, 65] which defines the Hansen sphere of each polymer such that solvents capable of dissolving the polymer will fall within the sphere. Solvents that can dissolve the polymer of interest are then identified by calculating the geometric distance (R_a)[63, 64] between the HSP values of the solvent and the polymer in Hansen space as shown in Equation 1 below.

$$R_a^2 = 4(\delta_{D_1} - \delta_{D_2})^2 + (\delta_{P_1} - \delta_{P_2})^2 + (\delta_{H_1} - \delta_{H_2})^2 \qquad (1)$$

Where R_a is the geometric distance between solvent and solute in Hansen space, δ_{D_1} and δ_{D_2} are the dispersion interaction HSPs for the solvent and solute, respectively, δ_{P_1} and δ_{P_2} are the polar interaction HSPs for the solvent and solute, respectively, and δ_{H_1} and δ_{H_2} are the hydrogen-bonding interaction HSPs for the solvent and solute, respectively.

Solvents with an R_a / R_0 ratio, known as the Relative Energy Difference (RED), less than one are expected to be able to dissolve the target polymer while solvents with a RED greater than one are expected to not be capable of dissolving the target polymer. Thus, potential solvents might be selected based on HSPs while those predicted to be incompatible may still be useful as antisolvents.

However, we emphasize that HSPs only provide an estimate of solubility of a target polymer in a given solvent, but generally the lower the RED the better. HSPs of the solvent compounds as well as selected polymers (calculated at 25 °C) were obtained using the HSPiP software (version 5.4.03).[64] It should also be noted that the HSPs of the selected polymers are only general approximations as actual results are resin-dependent for example low-density PE and high-density PE.

In addition to the calculation of HSPs, the HSPiP software also provides predictions for physical properties such as boiling point, water solubility (LogS), lipophilicity (LogP), critical properties, and Henry law constant as well as other quantities (a total of 55 properties). The LogS and LogP of the solvents are two of the important properties of a solvent when considering applications that involve dissolution and later precipitation of a solute. Thus, we sought to quantify the accuracy of HSPiP's LogS and LogP predictions against experimental data. For LogS, three datasets were used to validate HSPiP predictions, namely the ADME dataset,[66] the AqSolDB dataset,[67] and a LogS dataset curated by Zang et al.,[68] containing 1,290, 9,100 and 2,100 molecules along with their corresponding experimental LogS values, respectively. For LogP, two datasets were used to validate HSPiP predictions, namely, a LogP dataset curated by Zang et al.,[68] and a LogP dataset curated by Alshehri et al., [69] containing 14,208 and 12,194 molecules and their corresponding experimental LogP values, respectively.

2.1.4. Machine Learning (ML) prediction of LogS and LogP

Due to the poor prediction of the LogS and LogP (See Figure S1-S2), we have built neural network (NN) models to predict the LogS and LogP values of the studied potential solvent molecules, using fully connected dense layers and descriptors produced by the HSPiP software. For prediction of LogS, the ADME,[66] AqSolDB,[67] and Zang[68] datasets were used to train and

validate our model. Similarly, for the prediction of LogP, the Zang,[68] and Alshehri[69] datasets to train and validate the NN.

2.1.4.1. Data Preparation and Model Training

NN models typically require the input data be preprocessed in various ways, for example the removal of missing values, normalization of inputs, and feature selection, in order to prevent biasing of the model towards descriptors with large values in addition to making model training more efficient.[70] To preprocess the raw HSPiP descriptor data, first we removed rows which contained "NaN" values. NaN values were present for compounds in the training data for which HSPiP was unable to process due to either having a metal, having a complex SMILES string, or for compounds with dotted SMILES representations such as salts (e.g. [Na+].[Cl-]). Next, the HSPiP descriptors were converted into array format and scaled using the standard scaler function of the sklearn package in python.[71] This is used to resize the distribution of values for each descriptor such that the mean is zero and the standard deviation is one. Next, we performed Principal Component Analysis (PCA)[72] on the training data to reduce dimensionality of the data, followed by a random train/test splitting of the data. In this work, we have also considered the effect of training set size on the performance of the model and consequently tested an 80/20 and 90/10 train/test split (Table S3-S8). In order to find an optimal architecture, we have tested six different architectures described below, and compared their performance in predicting LogS and LogP values against experimental data. For the training of these models, we used the stochastic gradient descent (SGD)[73] optimizer as implemented in Tensorflow,[74] while reserving 10% of the training set as a validation set. To prevent over-fitting, we defined an early-stopping criterion which stopped the training of the model if the validation loss did not improve for 5 epochs, and because of this none of the models were trained for more than 500 epochs. After the training of

each model was complete, the best models were saved, and their performance were evaluated on the test set using metrics previously defined. Building, training, and evaluation of models were performed using Tensorflow[74] on Google Colab[75] which is a free Google service linked to Google Drive account. (Scripts used in this work are provided in our GitLab repository: https://gitlab.com/szilvasi-group/logs_logp-prediction).

2.1.4.2. Model Architecture

In this work, we developed neural network models which have been shown to be capable of predicting properties of organic molecules.[76-79] We trained a number of different models in which we varied the number and type of hidden layers as well as type of activation function in their architecture so as to obtain a relatively optimal model.

Model 1 consists of six dense layers, with 512, 512, 256, 256, 128, and 1 neuron(s) each. Model 2 is made up of ten layers, with six dense layers with the ReLU activation function,[80] and four dropout layers, which zero out the output of a certain fraction of neurons of the preceding layer to prevent overfitting.[81] For Model 2, the first eight layers are made of alternating dense (with the ReLU activation function) and dropout layers with 512 neurons, 30% dropout, 512 neurons, 30% dropout, 256 neurons, 20% dropout, 256 neurons, and 20% dropout, respectively. The final two dense layers contain 128, and 1, neuron(s), respectively. Model 3 is built up from ten layers, with six dense layers (using the ReLU activation function), and four batch normalization layers, which standardizes the output of the preceding layer. For Model 3, the first eight layers are made of alternating dense and batch normalization layers with the dense layers (using the ReLu activation function) containing 512 neurons, 512 neurons, 256 neurons, 256 neurons, respectively. The final two dense layers contain 128, and 1, neuron(s), respectively. Model 4 has fourteen layers, with six dense layers (using the ReLU activation function), four batch normalization layers, and four

dropout layers in total. For Model 4, the first twelve layers are divided into four blocks each consisting of three layers – a dense layer, followed by a batch normalization layer, and finally a dropout layer. In the first block, the dense layer contains 512 neurons, followed by the dropout layer with 30% dropout. In the first and second blocks, the dense layers contain 512 neurons each while the dropout layers perform 30% dropout. The dense layers in the third and fourth blocks contain 256 neurons each, while the dropout layers perform 20% dropout. The final two dense layers contain 128, and 1, neuron(s), respectively. Model 5 has the same architecture as Model 4 but uses the LeakyReLU activation function.[82] Finally, Model 6 has the same architecture as Model 5 but with an additional block of dense (1024 neurons), batch normalization, and dropout (40% dropout) layers as the first 3 layers of the model in addition to a 5% dropout layer preceding the final dense layer (1 neuron).

2.1.5. ML prediction of Melting Point

Due to the poor prediction of the melting point (see Figure S3), the melting point of compounds have been calculated using the directed message parsing neural network (D-MPNN) model, which is a 2D graph convolutional model that has been shown to shown to perform well on various tasks.[83-85] The D-MPNN was used to learn the contribution of each atom in the molecule to the melting point of the molecule. The implementation of the D-MPNN model as well as atom and bond features in this work followed the original Chemprop model developed by Yang et al.,[83] details for which can be found in the original paper by Yang et al.[86] The Chemprop model encodes the atomic features such as atom type, number of bonds, formal charge, chirality, number of hydrogens, hybridization, aromaticity, and atomic mass.[87] Two datasets were used to train the Chemprop model, namely the Bradley dataset,[88] and an melting point dataset collected by Zang et al.,[68] containing 3,041, and 8,648 molecules along with their experimental melting point values,

respectively. After removing duplicates, the final dataset contained 11,324 molecules. We also considered the effect of the training set size on the model performance and considered an 80/10/10, and 90/5/5 train/validation/test split (see Table S13). Default settings for the Chemprop model were used and training was done for 30 epochs. To find glycerol-like molecules on which to evaluate the reliability of our trained model to give accurate predictions for our catalogue of glycerol-derived solvents, we first collected a small set of glycerol-like molecules (See Supporting Information). Next, we collected a diverse dataset containing organic, and drug-like compounds curated by Tetko et al.[89] from which we collected glycerol-like molecules. By using a similarity function provided with the Chemprop model based on Morgan fingerprint[90] similarity, we extracted 232 glycerol-like molecules from the Tetko et al. dataset[89] which was used as an external test set (See Figure S4 for performance of the final model in the external test set).

In our analysis, we will use the following metrics and abbreviations: mean absolute error (MAE), maximum absolute error (MAD), and root-mean-square error (RMSE). The metrics are defined as follows:

The error between predicted and experimental LogS/LogP values is defined as:

$$LogX' = LogX_{expt} - LogX_{HSPiP} \qquad (2a)$$

where $LogX'$ is the error, $LogX_{expt}$ is the experimental LogS or LogP value and $LogX_{HSPiP}$ is the LogS or LogP value predicted by HSPiP (X = S, P).

The error between predicted and experimental melting point values is defined as:

$$MP' = MP_{expt} - MP_{model} \qquad (2b)$$

where MP' is the error, MP_{expt} is the experimental melting point value and MP_{model} is the melting point predicted by the Chemprop model.

The MAE is defined as:

$$\frac{\Sigma|LogX\prime|}{N} \quad (3a)$$

$$\frac{\Sigma|MP\prime|}{N} \quad (3b)$$

where N is the number of data points.

The MAD is defined as:

$$Max(|LogX'|) \quad (4a)$$

$$Max(|MP'|) \quad (4b)$$

The RMSE is defined as:

$$\sqrt{\frac{\Sigma(LogX_{HSPIP}-LogX_{expt})^2}{N}} \quad (5a)$$

$$\sqrt{\frac{\Sigma(MP_{model}-MP_{expt})^2}{N}} \quad (5b)$$

For calculated physical properties we define the mean and range as follows:

The mean is defined as:

$$Y_{mean} = \frac{\Sigma Y}{N} \quad (6)$$

and the range is defined as:

$$Y_{range} = Y_{max} - Y_{min} \quad (7)$$

where Y represents the property under consideration.

3. RESULTS AND DISCUSSION

We have calculated several physicochemical properties of our glycerol-derived solvents such as density, dipole moment, LogS, LogP, and melting point, and analyzed their compatibility with different polymers using HSPs. Below we will first discuss the physicochemical properties of each category of glycerol-derived solvents and explore the effect of different functional groups on the properties. To analyze the effect of functional groups, we form four subcategories for our analysis based on molecules that contain halogens (nitriles excluded), nitriles (with and without halogens), rings i.e. compounds containing cyclic or aromatic groups (halogen- and nitrile- containing

compounds excluded), and the last group named others encompasses all compounds without any of the aforementioned groups (i.e., contains hydrogen, amine, or alkyl/alkyl ether groups). Next, we will discuss the solubility of different polymers as predicted using HSPs and the effect of functional groups on the solubility of different polymers. Lastly, we will provide recommendations on the best solvent candidates based on their melting point and their predicted ability to dissolve various plastic materials.

3.1. Dipole Moment (μ)

The dipole moment can serve as a simple measure of the polarity of a molecule and helps to rationalize bulk and molecular properties such as melting and boiling points,[91] and have been shown to trend with the permittivity of glycerol-derivates.[39, 92] Moreover, the polarity of a solvent can be used to predict what kind of solutes will be soluble in the solvent, for example, polar solvents dissolve polar solutes.[93] Previous studies have demonstrated that functionalization of glycerol can produce molecules with a wide range of dipole moment values (both polar and non-polar).[32, 33, 35, 36, 39, 92] Figure 1a shows a probability density distribution for the dipole moment of each basic structure of glycerol-derivative, and from this we observe that a wide range of dipole moment is possible for each basic structure including polar and non-polar solvent candidates. GDA and GDK solvents have very similar distributions with a mean dipole moment of 2.75 D and 2.81 D, respectively, and ranges of 8.37 D and 9.82 D, respectively. For the GDEs and GDDs, the dipole moment values are higher with mean dipole moments of 3.20 D and 2.88 D, respectively, and ranges of 14.54 D and 10.78 D, respectively.

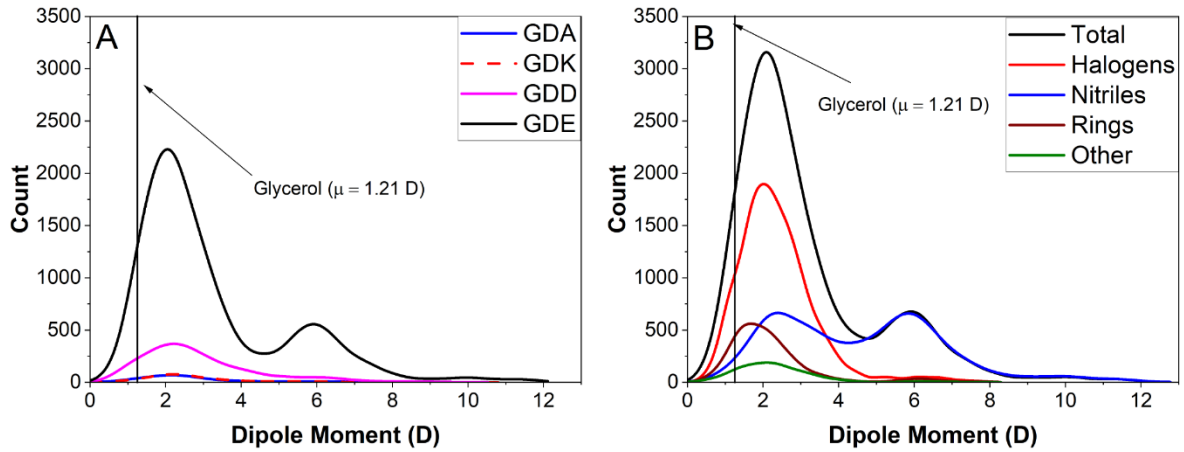

Figure 1. Probability density distribution of dipole moment for (a) GDA, GDK, GDD, GDE solvents and (b) glycerol-derived solvents based on subcategory. Vertical line indicates calculated dipole moment of glycerol.

Based on the wide range of dipole moment values for the studied glycerol derivatives, it is necessary to put the dipole moment in the context of common solvents that have been used for plastic dissolution such as MEK (calculated μ = 2.63 D) and acetone (calculated μ = 2.78 D). We note that 46% of the glycerol derivates have a greater dipole moment than MEK while 41% of the glycerol derivatives have a greater dipole moment than acetone. Additionally, compared to glycerol (calculated μ = 1.21 D), 93% of the glycerol derivatives have a greater dipole moment. This means that there are numerous potential options for the dissolution of ionic, polar solutes or non-polar solutes in our catalogue of glycerol derivates. In addition, we also highlight that the GDE distribution has two peaks (2.04 D and 5.90 D). We find in Figure 1b that the peak at 5.90 D is the result of the nitriles subcategory while the peak at 2.04 D predominately consists of halogen containing molecules. Specifically, the bimodal nature of the distribution for the nitriles subcategory is related to the size of the cyano- containing moiety. By manually inspecting the data set, we find that molecules in the nitriles group with dipole moment around 2 D are typically those molecules which have a CH_2CN group while solvents with dipole moment around 5.9 D are those

molecules with PhCN and PhPhCN groups. This trend can be explained by the larger distance between the polar CN and the ether ends of the molecules[94] and the larger polarizability of the phenyl rings that also increases the dipole moment.[94-97] Overall, we find that the nitriles subcategory, on average, produces the most polar solvents (mean μ = 4.66 D), followed by the halogens subcategory (2.38 D), the others (2.41 D), and rings (2.20 D) subcategories, respectively.

3.2. LogS and LogP Solubility

The LogS and LogP are important properties to predict what solvation processes the solvents can be used for. LogS is a measure of the solubility of a compound in water and is defined as the maximum amount of solute a given volume of water can dissolve,[67] meanwhile LogP, also known as octanol/water coefficient, represents the equilibrium ratio of a compound between an octanol and a water phase and is thus a measure of how hydrophilic or hydrophobic a compound is.[98] LogS and LogP are measures that can indicate the behavior of a compound in various applications, for example in drug design or plastic waste degradation.[67, 99] Based on the accuracy of our best NN for LogS prediction (MAE: 0.54, RMSE: 0.76) as shown in Figure S1and Table S1, we predicted the LogS value for each glycerol derived solvent. Figure 2a shows the probability density distribution of the LogS values of the glycerol derivates. From the NN generated LogS values, we find that majority of the glycerol-derivates are insoluble in water as seen for other studies of glycerol-derivaties previously.[33-36] Molecules miscible in water (Logs > 0) contain -OH groups and thus the higher solubility can be attributed to higher propensity for hydrogen bonding. On average, the GDA and GDK solvents have the best solubility in water with mean LogS values of -1.45, and -1.40, respectively, while the GDE and GDD solvents are predicted to be much less soluble with mean LogS values of -2.62, and -2.24, respectively. To provide more insight into how the attached functional groups affect water solubility of the glycerol derivates, we also provide the

probability density distribution of the LogS values of the glycerol derivatives based on subcategory in Figure 2b. Here, we observe that the molecules containing alkyl ethers (others category) are the most soluble in water with a mean LogS of -0.33, while the glycerol derivates containing halogens, nitriles, and rings are less water soluble on average with mean LogS value of -2.24, -3.37, and -1.97, respectively. While previous studies have reported the general hydrophobicity of glycerol derivates, they have also demonstrated that the presence of hydrophilic alkyl ether or -OH groups tends to enhance the water solubility of glycerol derivatives[32-34, 36] which we also observe here.

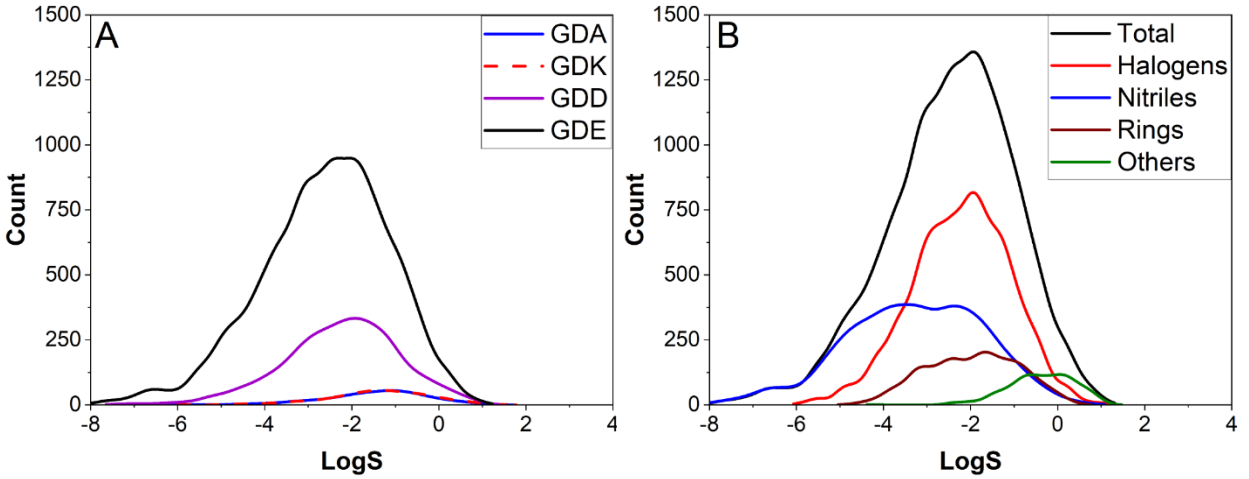

Figure 2. Probability density distribution of LogS for (a) GDA, GDK, GDD, GDE solvents and (b) glycerol-derived solvents based on subcategory.

Based on the accuracy of our best NN for LogP prediction (MAE: 0.25, RMSE: 0.37) as shown in Figure S2 and Table S2, we predicted the LogP value for each glycerol derived solvent. Figure 3a shows the probability density distribution of the LogP values of the glycerol derivates. From the NN generated LogP values, we find that the majority of the glycerol-derivates are hydrophobic in nature as seen in other studies of glycerol-derivatives.[32, 33, 36] Overall, the GDE and GDD solvents are most hydrophobic with mean LogP values of 2.90, and 2.36, respectively, while the GDA and GDK solvents are less hydrophobic with LogP values of 1.29, and 1.51, respectively. We also highlight the presence of two shoulders in the distribution of LogP values for the GDE

solvents (4.2, and 6.8). In Figure 3b, we show the probability density distribution of the LogP values of the glycerol derivatives based on subcategory. Based Figure 3b, we can explain the shoulders in the distribution for the GDE solvents by the nitriles and halogens subcategories, specifically molecules containing one or more CF_3 groups which are known to be hydrophobic.[100, 101] Overall, for the different subcategories we note the opposite trend compared to the LogS wherein the most hydrophobic category (nitriles) is the least water soluble i.e., others (mean LogP: 0.55) < rings (mean LogP: 1.88) < halogens (mean LogP: 2.89) < nitriles (mean LogP: 3.01).

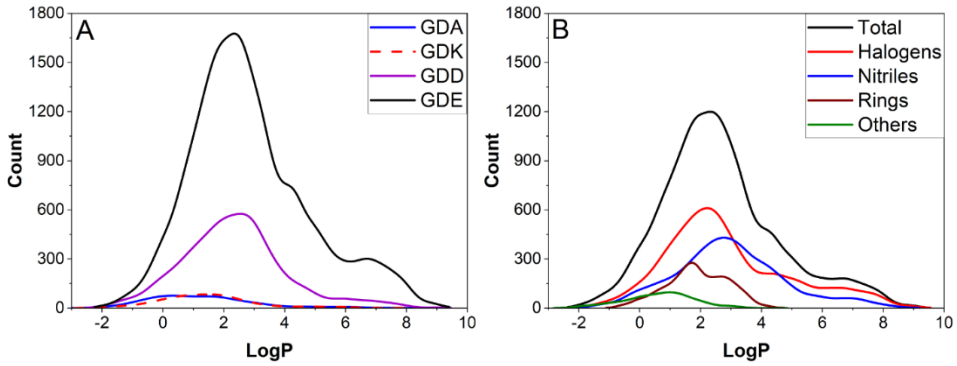

Figure 3. Probability density distribution of LogP for (a) GDA, GDK, GDD, GDE solvents and (b) glycerol-derived solvents based on subcategory.

As we have seen, the hydrophobicity/philicity for glycerol derivates can be tuned based on the selection of fucntional groups. In addition to this, we were also interested in molecules which are both soluble in water (LogS > 0) and lipophilic (LogP > 0). By manually filtering the dataset, we find 91 solvent candidates (See Table S9) which exhibit both solubility in water and lipophilicity with average LogS and LogP values of 0.22, and 0.56, respectively, in addition to ranges of 0.7, and 1.42. Figure 4 shows examples of molecules which exhibit this behaviour from each of the GDA, GDK, GDE, and GDD categories. We also note that 70 of the 91 molecules contain an amine group which is known to promote soulubility in water and organic phases alike.[102, 103]

Considering the miscibility data, the studied glycerol derivates offer a broad range of options to choose from depending on requirements of hydrophilicity/hydrophobicity within the scope of the desired application.

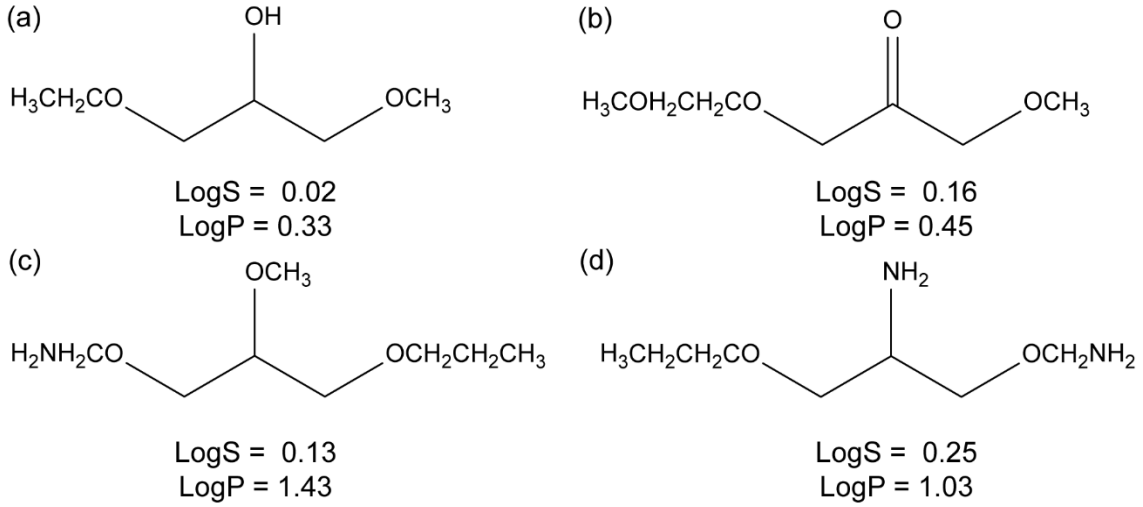

Figure 4. Example of a (a) GDA, (b) GDK, (c) GDE, and (d) GDD solvent that exhibit both water solubility (LogS > 0) and lipophilicity (LogP > 0).

3.3.Density (ρ)

Figure 5a shows a probability density distribution for the density of each basic structure of glycerol-derivative. From Figure 5a, we see that each category of glycerol-derivate has similar distributions of density with mean densities of 1.20, 1.22, 1.19, and 1.27 g/cm^3 and ranges of 2.40, 1.19, 2.35, and 2.04 g/cm^3 for the GDA, GDK, GDE, and GDD categories, respectively, compared to the density of glycerol (calculated ρ = 1.17 g/cm^3). In general, density trends in order of GDD > GDK > GDA > GDE. The increase in density from GDAs to GDKs can be explained by liquid contraction resulting from the loss of the hydroxyl group[33, 39] as indicated in the reduction of molar volume from GDA (mean molar volume: 191 cm^3/mol) to GDK (mean molar volume: 189 cm^3/mol). Therefore, even though GDAs have stronger intermolecular forces (i.e., hydrogen bonds), the conformational freedom of the rotatable hydroxyl group causes GDAs to have larger

free volume compared to GDKs. This means that for analogous GDAs and GDKs the reduced ability of GDKs to form hydrogen bonds is outweighed by the loss of free volume, hence GDKs are denser. However for GDEs, replacement of the hydroxyl group by an ether group leads to an increase in the molar volume (mean molar volume: 254 cm^3/mol) in addition to reduced dispersion interactions between molecules as a result of etherification which showed in the lower mean δ_d value for GDEs (17.08 $MPa^{0.5}$) compared to the other categories (GDAs: 17.26 $MPa^{0.5}$, GDKs: 17.35 $MPa^{0.5}$, GDDs: 17.17 $MPa^{0.5}$).

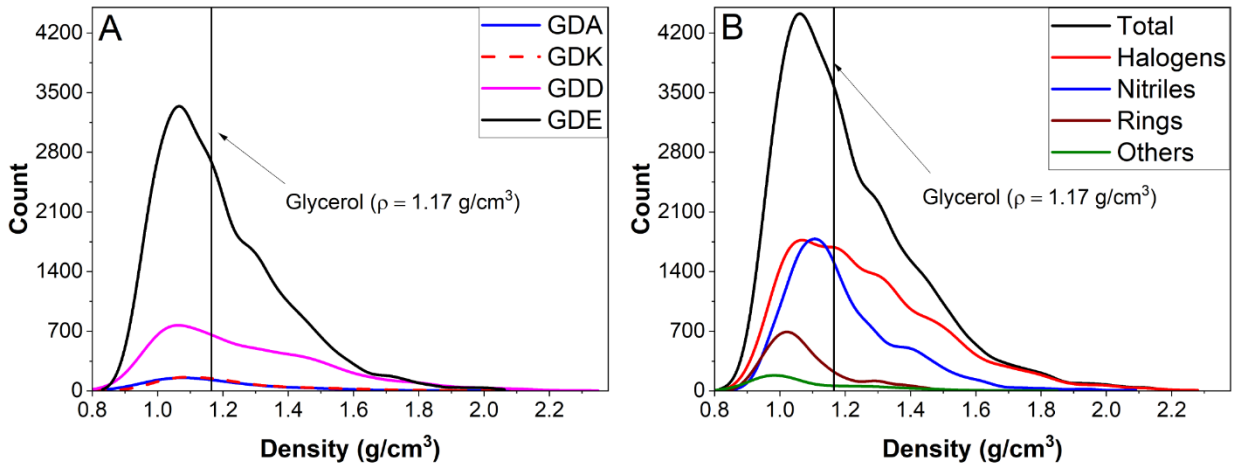

Figure 5. Probability density distribution of density for (a) GDA, GDK, GDD, GDE solvents and (b) glycerol-derived solvents based on subcategory. Vertical line indicates calculated density of glycerol.

For each category of glycerol derivate, the most dense compounds are those containing one or more -CH_2I or -CH_2Cl groups, with the density of 3.30, 2.12, 2.63, and 2.43 g/cm^3 for the most dense solvents in the GDA, GDK, GDE, and GDD categories, respectively, which is attributed to the high atomic mass of halogen atoms. Thus, the large mean density of 1.27 g/cm^3 for the GDDs is potentially due to the presence of heavy halogen atoms such as bromine and iodine. We also note that the long tails of the density distributions for each category in Figure 5a is also because of those solvents that contain halogen atoms such as F, Cl, and Br which due to their high atomic

mass significantly increase the density of the solvents. Figure 5b shows probability density distributions for the studied solvents grouped in subcategories. Here, we observe that for solvents that contain either only rings or alkyl/alkyl ether groups (i.e., others subcategory), almost the entire range of densities (81% of rings, and 73% of others) fall below the density of glycerol (calculated $\rho = 1.17$ g/cm^3) and have density similar to those of glycerol-derivates in literature, for example glycerol monoethers (0.96 – 1.36 g/cm^3) and triethers (0.85 – 1.30 g/cm^3).[34, 36, 92] For the different subcategories we observe mean densities of 1.27, 1.20, 1.08, and 1.09 g/cm^3, and ranges of 3.30, 1.72, 0.87, and 1.13 g/cm^3 for the halogens, nitriles, rings, and others subcategories, respectively.

3.4. Melting Point

The melting point is critical for solvent design as the predicted solvents should be in liquid state at room temperature for economic dissolution processes. We have calculated the melting point using the Chemprop code[83] as described in the Computational Methods. Figure 6a shows a probability density distribution for the melting point of each basic structure of glycerol-derivative, and from this we observe that a wide range of melting points for the studied glycerol derivatives. On average, GDA, GDD, and GDE solvents are predicted to be liquid indicated by mean melting points of 14 °C, 2 °C, and 4 °C, respectively, while the GDK solvents are predicted to be solid with mean melting point of 56 °C. We also highlight the presence of a second peak for the GDE distribution (centered at 130 °C) as well as long tails for the GDA, GDK, and GDD categories. The second peak at 130 °C in the GDE distribution as well as the long tails for all categories are as a result of the nitriles subcategory (Figure 6b). Here, solvents containing the bulky PhPhCN groups have the highest predicted melting points resulting in an average melting point of 61 °C for the nitriles subcategory compared to -23 °C, -11 °C, and -25 °C for the halogens, rings, and the others

subcategories, respectively. Overall, we find that 74% of the studied glycerol derivates (7131 solvents) are predicted to be liquid at room temperature (25 ˚C).

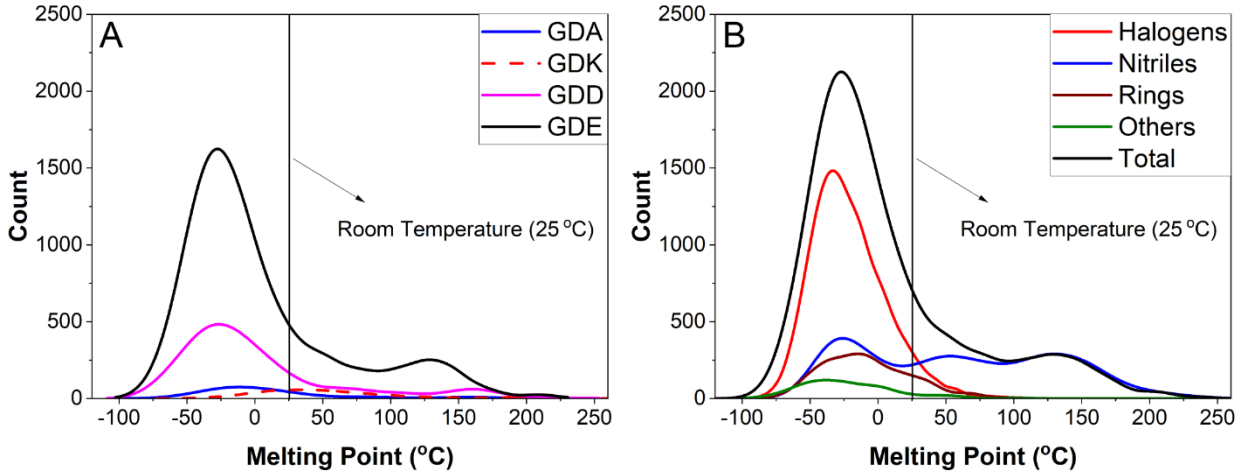

Figure 6. Probability density distribution of melting point for (a) GDA, GDK, GDD, GDE solvents and (b) glycerol-derived solvents based on subcategory. Vertical line indicates room temperature.

3.5. RED Analysis

The key to the successful implementation of a solvent-based plastic recycling process is the preselection of a solvent that is capable of selective dissolution of the target plastic material. However, given the variety of plastic materials and large number of solvent candidates presented in this study, solvent selection based on experimental screening alone is not possible. In this section, we show that glycerol-derived solvents can be found for polar and non-polar plastic materials based on the calculation of HSPs.

Figure 7a shows probability density distributions of the RED values of the studied solvents for non-polar plastics – PE, PP, and PS. The studied glycerol derivates perform best for PS on average with a mean RED of 0.76 and 7941 solvents with an RED below 1. Interestingly, compared to p-cymene (RED = 0.40) which is another green solvent for PS dissolution,[27, 28] there are 850 glycerol derivates with RED values below that of p-cymene. For PE and PP, the glycerol derivates perform worse with average RED values of 0.99 and 1.20, respectively, and only 5491 and 2813 solvents, respectively, with an RED below 1. We also highlight that the studied glycerol derivates outperform glycerol in terms of the RED for non-polar plastics (RED_{PE} = 3.48, RED_{PP} = 3.71, RED_{PS} = 3.28) and polar plastics (RED_{PES} = 3.05, RED_{PET} = 2.77, RED_{PVC} = 2.73).

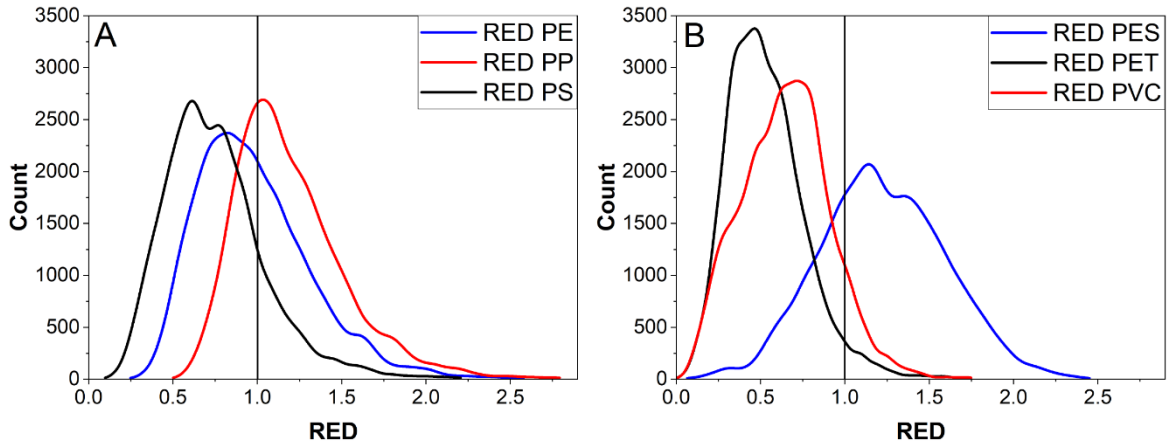

Figure 7. Probability density distribution of RED for (a) non-polar plastics, and (b) polar plastics. Vertical black lines represent the threshold (RED = 1) above which solvents cannot dissolve the target plastic.

For polar plastics (PES, PET, and PVC, Figure 7b), the RED analysis predicts numerous glycerol derivative candidates for the dissolution of PET and PVC. We observe an average RED of 0.54 and 0.65 for PET and PVC, respectively. In addition, we have majority of the solvents with a RED below 1 (PVC: 8700 and PET: 9199) and a narrow range of RED values (PVC: 2.68 and PET: 2.74). For PES, the glycerol derivatives are predicted to excel less with an average RED of 1.23

and much wider range of 3.00. The relatively poor performance of the glycerol derivatives is due to the unique nature of PES in terms of its HSPs. Because of the presence of the benzene rings, ether, and sulfone groups in its structure, PES has high δ_d, δ_p, and δ_h in addition to having a small Hansen radius. When compared to the HSPs of the other plastic materials considered here as shown in Table 1, finding appropriate solvents for PES that balance the HSPs will be more difficult and as such we only have 1595 solvents predicted to be able to dissolve PES based on RED.

Table 1. Calculated HSPs of selected plastic materials.

Plastic	δ_d	δ_p	δ_h	R_0
PVC	18.8	9.2	6.3	8.0
PES	19.6	10.8	9.2	6.2
PP	18.0	0.0	1.0	8.0
PET	18.2	6.4	6.6	8.0
PE	16.9	0.8	2.8	8.0
PS	18.5	4.5	2.9	8.0

To provide more information on the effect of functional groups in dissolution of the selected plastic materials, Figure 8 show probability density distributions for the RED values of our solvents grouped by subcategory for the studied plastics.

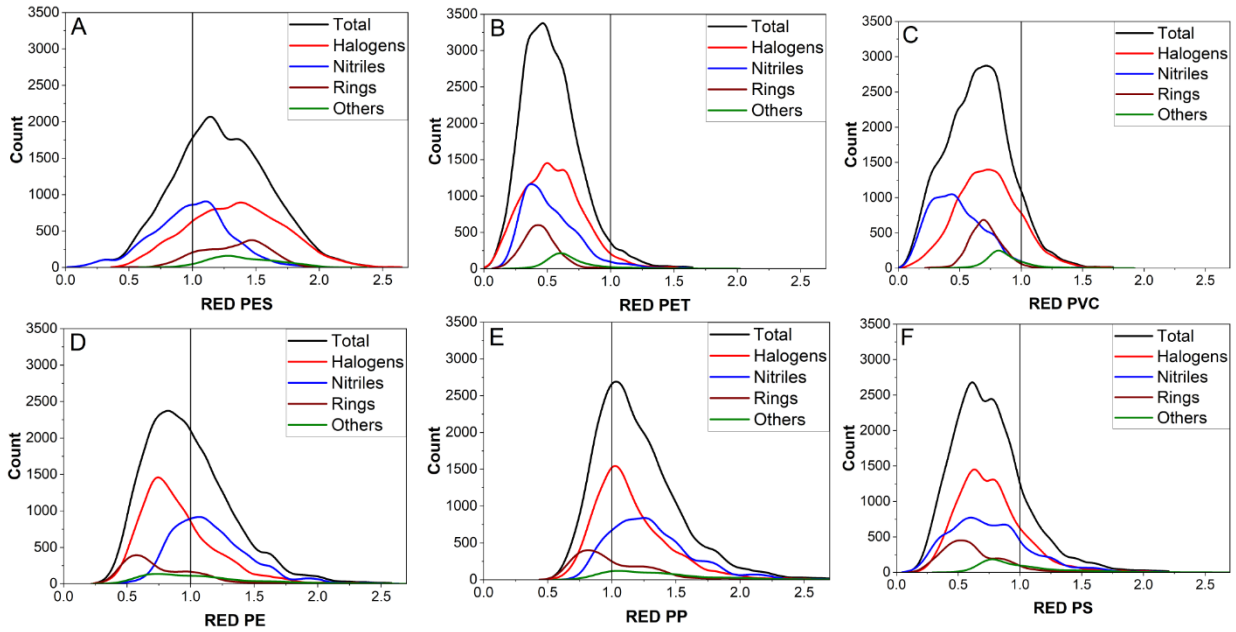

Figure 8. Probability density distribution of RED for (a) PES, (b) PET, (c) PVC (d) PE, (e) PP, and (f) PS for the studied glycerol-derived solvents based on subcategory. The distribution of the entire dataset is also disclosed. Vertical black lines represent the threshold (RED = 1) above which solvents cannot dissolve the target plastic.

For the dissolution PES, the nitriles and halogens subcategories give the best performance (mean RED of 0.98 and 1.35, respectively) which we attribute to the presence of highly polarizable groups such as I, Br, PhCN or PhPhCN. We also note that the best solvents for PES usually contain a hydroxyl group in addition to one of the aforementioned groups which give a good combination of HSPs that are similar to that of PES. For example, the best overall glycerol derivative for PES (RED = 0.05) is a GDA solvent which contained a CH_2I and a PhCN group (See Figure 9). For the rings subcategory, while having solvents with high δ_d and δ_h in some cases, the absence of polar groups resulted in a mean RED of 1.33. Interestingly, there are two peaks centered at 1.04 and 1.48 which indicate that certain groups of molecules in the subcategory perform better than others. Solvents clustered around 1.04 were again typically GDAs or other molecules containing a hydroxyl group, while the solvents clustered at 1.48 were generally GDEs and GDDs. By manually

inspecting the dataset, we observe that the best solvents (RED < 1) for PES in the ring subcategory are GDA with either benzyl or cyclohexyl groups, and GDK molecules with hydroxyl or amine groups. While the worst performing molecules are GDK molecules without any additional polar groups or GDE and GDD molecules regardless of the attached groups. The poor performance of GDEs and GDDs can be rationalized by the reduction in the δ_p and δ_h with etherification or deoxygenation. While for poorly performing GDAs and GDKs, their performance is explained by the lack of hydrogen bond donor ability and the presence of nonpolar cyclic groups which reduce the overall polarity of the molecule.

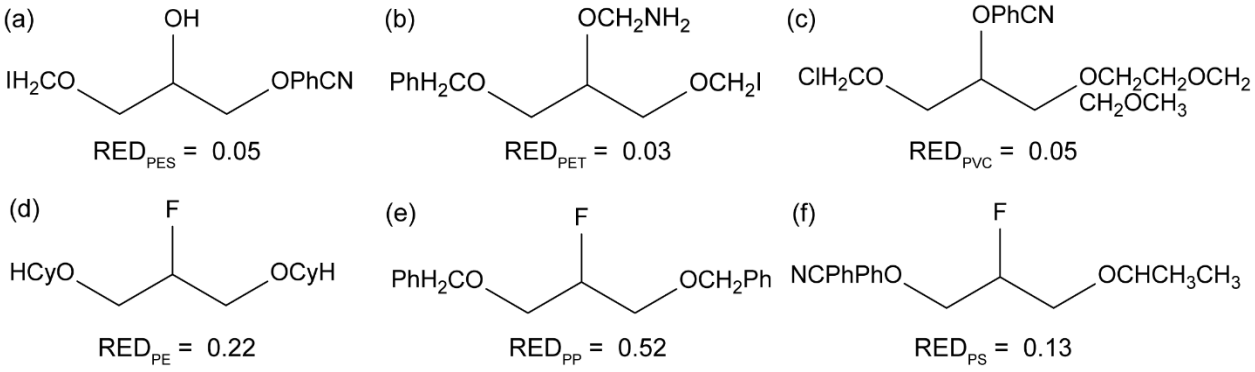

Figure 9. Glycerol-derived solvent with the lowest RED value for (a) PES, (b) PET, (c) PVC, (d) PE, (e) PP, and (f) PS.

In the case of PET, all subcategories produce solvents which are predicted to dissolve PET with all subcategories having mean RED values below 1 (halogens: 0.55, nitriles: 0.53, rings: 0.45, and others: 0.72) and their distribution of RED clustered below 1. This can be attributed to the structural similarity between PET and the glycerol derivates in terms of the presence of ether and ketone groups such that the HSPs are close. Overall, PET has the largest proportion of possible solvents with 9,214 glycerol solvents having an RED less than 1, while the best solvent candidate for PET (RED = 0.03) is a GDE that contains a CH_2I, a Ph group, and a CH_2NH_2 group (See Figure 9). This is particularly promising since PET is abundant in post-consumer waste streams.[104]

Likewise, for dissolving PVC we find potential solvents regardless of the attached functional group. Nonetheless, the nitriles subcategory provide the best performance with mean RED of 0.47 and range of 2.14, followed by the rings subcategory with average RED of 0.71 and a range of 1.09 while the halogens and others subcategories have average REDs of 0.73 and 0.90, respectively, and ranges of 2.09 and 2.14, respectively, with the best solvent for PVC (RED = 0.05) being a GDE containing a CH_2Cl, a PhCN, and a $CH_2CH_2OCH_2CH_2OCH_3$ group (See Figure 9). We also highlight that while glycerol derivates containing explicitly polar functional groups such as PhCN or PhPhCN may perform better for PVC dissolution, some glycerol derivates containing nominally non-polar functional groups such as benzyl groups may also be used as a result of dispersive and hydrogen bonding interactions. Thus, the good performance of molecules in the nitriles subcategory is largely because those molecules with PhCN or PhPhCN groups which maximize polar and dispersive interactions with PVC as a result of the polar cyano group, and large the Ph and PhPh groups that are involved in the dispersion interactions.

Conversely, even though the Hansen radius of PE and PP is comparable to that of the polar plastics (Table 1), the polar, and hydrogen bonding parameters do not play a significant role in determining which solvents can dissolve them. Thus, solvents with polar groups and an appreciable δ_p and/or δ_h value are likely to lie outside the Hansen sphere of the plastic material. This means that for PE and PP, glycerol derivates containing non-polar functional groups with high δ_d and low δ_p and δ_h values will perform best. Consequently, glycerol derivates in the rings subcategory perform best with an average RED value of 0.77, while the halogens, others and nitriles subcategories have an average RED of 0.90, 1.11, and 1.17, respectively. In general, the best solvents for PE are the low dipole moment GDE and GDD solvents with cyclic/aromatic groups attached with the exception of a few GDKs which contain only cyclic functional groups. This

indicates that high hydrogen bonding ability of the GDAs and GDKs negatively impacts the ability of the solvent to dissolve PE even if the solvent contains a cyclic or aromatic group. It should also be noted that the best glycerol derivate for PE (RED = 0.22) is a GDD that contains two CyH groups attached to the terminal ether positions, and a fluorine atom in the X position (See Figure 9). Analogous to PE, the glycerol derivates predicted to dissolve PP are solvents in the rings subcategory, however the glycerol derivates perform slightly worse on average for PP compared to PE with an average RED values of 1.01, 1.15, 1.31, and 1.40 for the rings, halogens, nitriles, and others subcategories, respectively. In addition, the best glycerol derivates for PP dissolution are the low dipole moment GDEs and GDDs, in addition to a few GDKs, with cyclic/aromatic groups attached (See Figure 9). This again emphasizes the negative effect of the hydrogen bonding ability on the capacity of GDAs and GDKs to dissolve PP. For example, the best solvent for PP (RED = 0.52) which is a GDD solvent that contains two Ph groups attached to the terminal ether positions, and a fluorine atom in the X position (See Figure 9)

In contrast to PE and PP, a variety of glycerol derivates with different functional groups (both polar and non-polar) are predicted to be able to dissolve PS. The glycerol derivates within the rings subcategory are on average the best for dissolving PS with mean RED values of 0.76, 0.75, 0.62, and 1.04 for the halogens, nitriles, rings, and others subcategories, respectively. Generally, the best glycerol derivatives for PS are GDEs, and GDDs that do not contain any -OH groups, in addition to a few GDKs that contain cyclic/aromatic functional groups which again emphasizes the negative effect of hydrogen bonding. For example, the best glycerol derivate for PS (RED = 0.13) is a GDD solvent that contains a PhPhCN and an isopropyl group in addition to a fluorine atom in the X position (See Figure 9).

3.6. RECOMMENDATIONS

Thus far, we have presented the physical properties of the glycerol-derived solvents as well as have analyzed their compatibility with selected polymers. To achieve selective plastic recovery, we recommend examples of solvents that are selective towards a specific polymer by considering the RED value and predicted melting point. We use the definition that a glycerol-derivative is selective for a particular plastic if the melting point is below 25 °C, the RED value for the particular plastic is below 1, the RED value for other plastics is above 1, and the difference between the RED value for that plastic (RED < 1) and the RED value for any other plastic (RED > 1) is at least 0.2. This definition is motivated by the simple rule of HSPs proposed by Hansen,[63, 64] and recent plastic recycling studies[12, 13] that have chosen solvents based the RED value (above or below 1) of the solvent for the target polymer. Our definition also considers the limitations of HSPs in predicting solvent/non-solvents for polymer dissolution by defining a spread of at least 0.2. It has been shown in a previous study by Venkatram et al., that HSP has a prediction accuracy of 67% $\pm$ 10% for solvents and 76% $\pm$ 12% for non-solvents.[105] Prediction inaccuracy stems from the complex process of polymer solubility which involves swelling and diffusion in addition to being influenced by polymer structure, temperature and solvent concentration all of which are not captured by HSPs.[106] Due to the limitations of HSPs in predicting solvent/non-solvent especially in close calls (i.e., where RED is between 0.9 and 1), we cannot make conclusive statements about the solvent's ability to dissolve one plastic selectively over the other and thus we exclude them. Finally, the melting point criterion is introduced for practical reasons as economic plastic waste recycling should be done at room temperature.

Based on the abovementioned definition of selective solvents, we identify 11 solvents for PVC, 5 solvents for PET, and 32 solvents for PE (See Table S10-S12 for RED and melting point). To

illustrate, Figure 10 shows the solvent with lowest RED for PE, PET, and PVC based on the RED, and melting point.

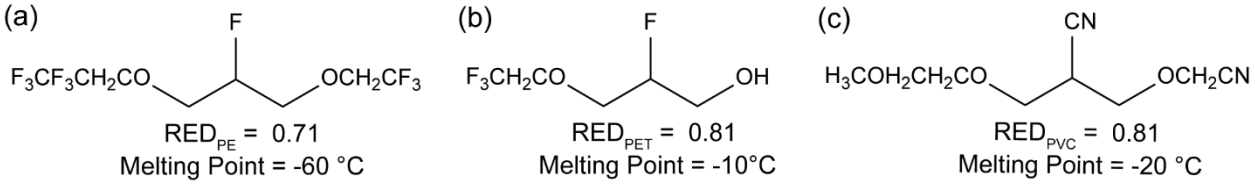

Figure 10. Glycerol-derived solvent examples for the selective dissolution of (a) PE, (b) PET, and (c) PVC based on calculated RED and melting point criteria.

For the dissolution of PES, PP, and PS, there were no solvents that satisfied our definition for selection considering all six plastics. However, there are 376 and 2496 solvents which are selective towards PES, and PS, respectively, for a mixed feedstock of only PES, PP, and PS. While no solvents satisfy our selection criteria for PP even when only PES, PP, and PS are considered, there are 2268 solvents predicted to be able to dissolve PP (RED < 1 for PP, melting point < 25 °C) after the PES and PS fractions have been separated. Finally, we note that there are also 125 solvents which are predicted to be unable to dissolve any of the plastics considered here and can act as potential general anti-solvents (i.e., RED > 1 for all plastics, see Supporting Information).

Putting together our suggestions for solvents forms the basis for a process to separate a mixed feedstock containing PVC, PET, PE, PES, PP, and PS:

1. Selectively dissolve PVC fraction in a PVC selective solvent, and then separating the dissolved fraction from the PET, PE, PES, PP, and PS.
2. Selectively dissolve PET fraction in a PET selective solvent, and then separating the dissolved fraction from the PE, PES, PP and PS.
3. Selectively dissolve PE fraction in a PE selective solvent, and then separating the dissolved fraction from the PES, PP, and PS.

4. Selectively dissolve PES fraction in a PES selective solvent, and then separating the dissolved fraction from the PP, and PS.
5. Selectively dissolve PS fraction in a PS selective solvent, and then separating the dissolved fraction from the PP.
6. The remaining PP can then be dissolved in a non-selective solvent (RED < 1 for PP and one or more plastics). All the dissolved polymers can then be recovered by addition of antisolvent to the respective solutions.

Due to the complexity of plastic waste feedstocks, separating different polymers one after the other as described above may not be feasible. Consequently, first separating the feedstock into polar and non-polar fractions can be more tractable and may help reduce costs associated with sorting the waste plastic. Thus, we also devise an alternative plan for plastic waste recycling starting from that idea. To have greater reliability in the HSP-based predictions, we only consider solvents that have an RED < 0.6 for the target plastic(s) and RED > 0.9 all other plastics, in addition to having a melting point below 25 °C. Based on this, 7 solvents are predicted to dissolve the polar fraction (RED < 0.6 for PET, PES, PVC, and RED > 0.9 for PE, PP, and PS). Upon separating the polar and non-polar fractions, the polar fraction (PET, PES, and PVC) can be further used to recover PVC and PET simultaneously (RED < 0.6 for PET and PVC, RED > 0.9 for PES) before a further round of selective dissolution to recover each kind of polymer. For this, there are 1345 solvents that can dissolve PVC and PET simultaneously and separate them from PES, 7 solvents that can selectively dissolve PET from a mixture of PET and PVC (RED < 0.6 for PET, RED > 0.9 for PVC), and 52 solvents that can dissolve the remaining PES fraction (RED < 0.6 for PES). Similarly, for the non-polar fraction, there are 149 solvents that can dissolve PS (RED < 0.6 for PS, RED > 0.9 for PE and PP) from the non-polar fraction, 18 solvents to dissolve PE (RED < 0.6

for PS, RED > 0.9 for PP) from a mixture of PE and PP, and 14 solvents that can dissolve the remaining PP fraction.

A procedure to separate a mixed feedstock containing PVC, PET, PE, PES, PP, and PS first into polar and non-polar fractions, followed by recovery of each type of polymer, is thus based on combining our suggestions for solvents as outlined below:

1. Selectively dissolve polar fraction (PET, PES, PVC) in a solvent selective to only polar plastics, and then separating the dissolved polar fraction from the non-polar fraction (PE, PP, and PS).
2. Dissolve PET and PVC fraction in a PET and PVC selective solvent, and then separating the dissolved fraction from the PES.
3. Selectively dissolve PET fraction in a PET selective solvent, and then separating the dissolved fraction from the PVC. This is followed by the recovery of all the dissolved fractions by addition of anti-solvent to precipitate the polymers out of solution.

For the non-polar fraction:

1. Selectively dissolve PS fraction in a PS selective solvent, and then separating the dissolved fraction from the PE and PP.
2. Selectively dissolve PE fraction in a PE selective solvent, and then separating the dissolved fraction from the PP. Recovery of the dissolved PE, and PS fractions by addition of anti-solvent to the precipitate the polymers out of solution.
3. The remaining PP can then be dissolved in any non-selective solvent. The PE, PP, and PS polymers can then be recovered by addition of antisolvent to the respective solutions.

Our computational high-throughput screening framework can serve as a starting point for solvent development for plastic waste recycling, and as we have shown, the large catalogue of solvents

enables us to quickly preselect potential solvents for the target plastic(s) and devise plans for selective plastic waste recycling. To help the interested reader quickly filter through the glycerol-derived solvents to design their own recycling plan using additional user-defined selection criteria, for example excluding halogenated solvents or including metrics for toxicity and biodegradability, we provide the RED values of each solvent for each plastic as well as the predicted melting point in the Supporting Information in a format that facilitate such a selection process.

4. CONCLUSIONS

In this work, we have calculated the physicochemical properties (density, dipole moment, melting point, LogS, and LogP) of a catalogue of 9587 glycerol-derived solvents, in addition to evaluating their ability to dissolve different plastic materials namely PE, PET, PES, PP, PS, and PVC based on HSPs. In general, functionalization of glycerol produces glycerol-derivates provides with a wide range of properties for potential solvents for dissolving a variety of plastics. We have also provided examples of selective solvents for PE, PET, and PVC based on the RED and melting point, while we proposed a multi-step process for separating a mixed feedstock containing PES, PP, and PS. Additionally, we suggest a stricter solvent selection criterion based on RED, which formed the basis of a strategy to reduce costs associated with sorting waste plastics, whereby we separate the feedstock into polar and nonpolar fractions first before carrying out selective dissolution.

Traditional means of developing new solvents for plastic recycling are typically based on trial-and-error experimentation. Future work should focus on experimental validation of predicted physicochemical properties and solubilities of waste plastic materials for the most promising glycerol-derivate candidates. Additionally, our computational framework can be easily applied for new solvent systems that are based on other platform molecules as well as other plastic materials

not studied in this work. Moreover, computationally exploring large catalogues of solvent candidates will allow for the rational design of new solvent systems that can be used to process complex multicomponent plastic waste of almost any composition.

ASSOCIATED CONTENT

The data underlying this paper are available in the Supporting Information. The Supporting Information is available free of charge at the SI link.

Physical properties for all 9587 glycerol-derived solvents, and subcategories, HSPiP generated features for Log training data, HSPiP generated features for LogP dataset, HSPiP generated features for all 9587 glycerol-derived solvents, and glycerol-like molecules used to obtain test molecules RED and melting point for all 9587 solvents (XLSX)

RED and melting point for all 9587 solvents, selective solvents for each plastic using two different solvent selection criteria based on RED and melting point (XLSX)

Supplementary discussion on neural network prediction of Logs and LogP, supplementary table showing glycerol-derived solvents which are both lipophilic and water soluble, supplementary tables showing recommended solvents, parity plots showing predictive power of Chemprop model against HSPiP, and parity plot showing prediction of melting point for a set of glycerol-like molecules (PDF)

AUTHOR INFORMATION

Corresponding Author

*Tibor Szilvási – Department of Chemical and Biological Engineering, University of Alabama, Tuscaloosa, Alabama 35487, United States; Email: tibor.szilvasi@ua.edu

Author

Ademola Soyemi - Department of Chemical and Biological Engineering, University of Alabama, Tuscaloosa, Alabama 35487, United States

Author Contributions

The manuscript was written through the contributions of all authors. All authors have given approval to the final version of the manuscript.

Notes

The authors declare no competing financial interest.

Acknowledgements

A.S and T.S would like to acknowledge the financial support of the National Science Foundation (NSF) under grant number EFMA-2029387. Any opinions, findings, conclusions, and/or recommendations expressed in this material are those of the authors(s) and do not necessarily reflect the views of the NSF. A.S and T.S would also like to thank the University of Alabama and the Office of Information Technology for providing high-performance computing resources and support that has contributed to these research results. This work was also made possible in part by a grant of high-performance computing resources and technical support from the Alabama Supercomputer Authority.

REFERENCES

(1) Geyer, R.; Jambeck, J. R.; Law, K. L. Production, use, and fate of all plastics ever made. *Sci Adv* **2017**, *3* (7), e1700782. DOI: 10.1126/sciadv.1700782 From NLM.

(2) Geyer, R. *Production, Use and Fate of Synthetic Polymers. in Plastic Waste and Recycling*; Academic Press, Cambridge MA, USA. 2020, pp 13-32.

(3) Foundation, E. M. *Plastics and the Circular Economy*; https://archive.ellenmacarthurfoundation.org/explore/plastics-and-the-circular-economy (accessed 09/30/2022).

(4) Lim, X. Microplastics are everywhere - but are they harmful? *Nature* **2021**, *593* (7857), 22-25. DOI: 10.1038/d41586-021-01143-3 From NLM.

(5) Ragauskas, A. J.; Huber, G. W.; Wang, J.; Guss, A.; O'Neill, H. M.; Lin, C. S. K.; Wang, Y.; Wurm, F. R.; Meng, X. New Technologies are Needed to Improve the Recycling and Upcycling of Waste Plastics. *ChemSusChem* **2021**, *14* (19), 3982-3984, https://doi.org/10.1002/cssc.202101872. DOI: https://doi.org/10.1002/cssc.202101872 (acccessed 2022/09/30).

(6) Li, H.; Aguirre-Villegas, H. A.; Allen, R. D.; Bai, X.; Benson, C. H.; Beckham, G. T.; Bradshaw, S. L.; Brown, J. L.; Brown, R. C.; Cecon, V. S.; et al. Expanding plastics recycling technologies: chemical aspects, technology status and challenges. *Green Chemistry* **2022**, 24, 8899-9002, 10.1039/D2GC02588D. DOI: 10.1039/D2GC02588D.

(7) Triebert, D.; Hanel, H.; Bundt, M.; Wohnig, K. Solvent-Based Recycling. In *Circular Economy of Polymers: Topics in Recycling Technologies*, ACS Symposium Series, Vol. 1391; American Chemical Society, Washington DC, USA. 2021; pp 33-59.

(8) Sherwood, J. Closed-loop recycling of polymers using solvents. *Johnson Matthey Technology Review* **2020**, 4-15.

(9) Goto, M. Chemical recycling of plastics using sub- and supercritical fluids. *The Journal of Supercritical Fluids* **2009**, *47* (3), 500-507. DOI: https://doi.org/10.1016/j.supflu.2008.10.011.

(10) Rahimi, A.; García, J. M. Chemical recycling of waste plastics for new materials production. *Nature Reviews Chemistry* **2017**, *1* (6), 0046. DOI: 10.1038/s41570-017-0046.

(11) Pappa, G.; Boukouvalas, C.; Giannaris, C.; Ntaras, N.; Zografos, V.; Magoulas, K.; Lygeros, A.; Tassios, D. The selective dissolution/precipitation technique for polymer recycling: a pilot unit application. *Resources, Conservation and Recycling* **2001**, *34* (1), 33-44. DOI: https://doi.org/10.1016/S0921-3449(01)00092-1.

(12) Walker, T. W.; Frelka, N.; Shen, Z.; Chew, A. K.; Banick, J.; Grey, S.; Kim, M. S.; Dumesic, J. A.; Van Lehn, R. C.; Huber, G. W. Recycling of multilayer plastic packaging materials by solvent-targeted recovery and precipitation. *Sci Adv* **2020**, *6* (47), eaba759. DOI: 10.1126/sciadv.aba7599 From NLM.

(13) Sánchez-Rivera, K. L.; Zhou, P.; Kim, M. S.; González Chávez, L. D.; Grey, S.; Nelson, K.; Wang, S.-C.; Hermans, I.; Zavala, V. M.; Van Lehn, R. C.; et al. Reducing Antisolvent Use in the STRAP Process by Enabling a Temperature-Controlled Polymer Dissolution and Precipitation for the Recycling of Multilayer Plastic Films. *ChemSusChem* **2021**, *14* (19), 4317-4329,

https://doi.org/10.1002/cssc.202101128. DOI: https://doi.org/10.1002/cssc.202101128 (acccessed 2022/10/01).

(14) Sändig, K. Process for producing particularly stable condensation products, US2061635A, USA 1936.

(15) Young, D. W. S., W. J. Preparation of purified polyesters, US2491350, USA 1945.

(16) Wainer, E. Verfahren Zur Wiedergewinnung von Polyvinylchloridmaterialien Aus Abfall, DE2537297A1, DE, 1976.

(17) Mizumoto, Y. H., S. Process for processing disposed polymer mixture. JPS5229879A, JP, 1977.

(18) Seymour, R. B.; Stahl, G. A. Separation of waste plastics. An experiment in solvent fractionation. *Journal of Chemical Education* **1976**, *53* (10), 653. DOI: 10.1021/ed053p653.

(19) Achilias, D. S.; Giannoulis, A.; Papageorgiou, G. Z. Recycling of polymers from plastic packaging materials using the dissolution–reprecipitation technique. *Polymer Bulletin* **2009**, *63* (3), 449-465. DOI: 10.1007/s00289-009-0104-5.

(20) Achilias, D. S.; Roupakias, C.; Megalokonomos, P.; Lappas, A. A.; Antonakou, E. V. Chemical recycling of plastic wastes made from polyethylene (LDPE and HDPE) and polypropylene (PP). *Journal of Hazardous Materials* **2007**, *149* (3), 536-542. DOI: https://doi.org/10.1016/j.jhazmat.2007.06.076.

(21) Achilias, D. S.; Antonakou, E. V.; Koutsokosta, E.; Lappas, A. A. Chemical recycling of polymers from Waste Electric and Electronic Equipment. *Journal of Applied Polymer Science*

2009, *114* (1), 212-221, https://doi.org/10.1002/app.30533. DOI: https://doi.org/10.1002/app.30533 (acccessed 2022/10/05).

(22) Kartalis, C. N.; Poulakis, J. G.; Tsenoglou, C. J.; Papaspyrides, C. D. Pure component recovery from polyamide 6/6 6 mixtures by selective dissolution and reprecipitation. *Journal of Applied Polymer Science* **2002**, *86* (8), 1924-1930, https://doi.org/10.1002/app.11147. DOI: https://doi.org/10.1002/app.11147 (acccessed 2023/02/14).

(23) Mohan, M.; Keasling, J. D.; Simmons, B. A.; Singh, S. In silico COSMO-RS predictive screening of ionic liquids for the dissolution of plastic. *Green Chemistry* **2022**, *24* (10), 4140-4152, 10.1039/D1GC03464B. DOI: 10.1039/D1GC03464B.

(24) Zhou, P.; Sánchez-Rivera, K. L.; Huber, G. W.; Van Lehn, R. C. Computational Approach for Rapidly Predicting Temperature-Dependent Polymer Solubilities Using Molecular-Scale Models. *ChemSusChem* **2021**, *14* (19), 4307-4316, https://doi.org/10.1002/cssc.202101137. DOI: https://doi.org/10.1002/cssc.202101137 (acccessed 2023/02/14).

(25) Chandrasekaran, A.; Kim, C.; Venkatram, S.; Ramprasad, R. A Deep Learning Solvent-Selection Paradigm Powered by a Massive Solvent/Nonsolvent Database for Polymers. *Macromolecules* **2020**, *53* (12), 4764-4769. DOI: 10.1021/acs.macromol.0c00251.

(26) Sánchez-Rivera, K. L.; Zhou, P.; Kim, M. S.; González Chávez, L. D.; Grey, S.; Nelson, K.; Wang, S.-C.; Hermans, I.; Zavala, V. M.; Van Lehn, R. C.; et al. Reducing Antisolvent Use in the STRAP Process by Enabling a Temperature-Controlled Polymer Dissolution and Precipitation for the Recycling of Multilayer Plastic Films. *ChemSusChem* **2021**, *14* (19), 4317-4329, https://doi.org/10.1002/cssc.202101128. DOI: https://doi.org/10.1002/cssc.202101128 (acccessed 2022/10/01).

(27) Hattori, K.; Shikata, S.; Maekawa, R.; Aoyama, M. Dissolution of polystyrene into p-cymene and related substances in tree leaf oils. *Journal of Wood Science* **2010**, *56* (2), 169-171. DOI: 10.1007/s10086-009-1073-x.

(28) Shikata, S.; Watanabe, T.; Hattori, K.; Aoyama, M.; Miyakoshi, T. Dissolution of polystyrene into cyclic monoterpenes present in tree essential oils. *Journal of Material Cycles and Waste Management* **2011**, *13* (2), 127-130. DOI: 10.1007/s10163-011-0005-1.

(29) Gutiérrez, C.; García, M. T.; Gracia, I.; de Lucas, A.; Rodríguez, J. F. Recycling of extruded polystyrene wastes by dissolution and supercritical CO2 technology. *Journal of Material Cycles and Waste Management* **2012**, *14* (4), 308-316. DOI: 10.1007/s10163-012-0074-9.

(30) Noguchi, T.; Miyashita, M.; Inagaki, Y.; Watanabe, H. A new recycling system for expanded polystyrene using a natural solvent. Part 1. A new recycling technique. *Packaging Technology and Science* **1998**, *11* (1), 19-27, https://doi.org/10.1002/(SICI)1099-1522(199802)11:1<19::AID-PTS414>3.0.CO;2-5. DOI: https://doi.org/10.1002/(SICI)1099-1522(199802)11:1<19::AID-PTS414>3.0.CO;2-5 (acccessed 2022/10/02).

(31) Milescu, R. A.; Zhenova, A.; Vastano, M.; Gammons, R.; Lin, S.; Lau, C. H.; Clark, J. H.; McElroy, C. R.; Pellis, A. Polymer Chemistry Applications of Cyrene and its Derivative Cygnet 0.0 as Safer Replacements for Polar Aprotic Solvents. *ChemSusChem* **2021**, *14* (16), 3367-3381, https://doi.org/10.1002/cssc.202101125. DOI: https://doi.org/10.1002/cssc.202101125 (acccessed 2022/10/02).

(32) Qian, S.; Liu, X.; Dennis, G. P.; Turner, C. H.; Bara, J. E. Properties of symmetric 1,3-diethers based on glycerol skeletons for CO2 absorption. *Fluid Phase Equilibria* **2020**, *521*, 112718. DOI: https://doi.org/10.1016/j.fluid.2020.112718.

(33) Qian, S.; Liu, X.; Turner, C. H.; Bara, J. E. Glycerol-derived solvents containing two or three distinct functional groups enabled by trifluoroethyl glycidyl ether. *AIChE Journal* **2022**, *68* (3), e17533, https://doi.org/10.1002/aic.17533. DOI: https://doi.org/10.1002/aic.17533 (acccessed 2022/10/02).

(34) García, J. I.; García-Marín, H.; Mayoral, J. A.; Pérez, P. Green solvents from glycerol. Synthesis and physico-chemical properties of alkyl glycerol ethers. *Green Chemistry* **2010**, *12* (3), 426-434, 10.1039/B923631G. DOI: 10.1039/B923631G.

(35) Qian, S.; Liu, X.; Emel'yanenko, V. N.; Sikorski, P.; Kammakakam, I.; Flowers, B. S.; Jones, T. A.; Turner, C. H.; Verevkin, S. P.; Bara, J. E. Synthesis and Properties of 1,2,3-Triethoxypropane: A Glycerol-Derived Green Solvent Candidate. *Industrial & Engineering Chemistry Research* **2020**, *59* (45), 20190-20200. DOI: 10.1021/acs.iecr.0c03789.

(36) Qian, S.; Liu, X.; Turner, C. H.; Bara, J. E. Synthesis and properties of symmetric glycerol-derived 1,2,3-triethers and 1,3-diether-2-ketones for CO2 absorption. *Chemical Engineering Science* **2022**, *248*, 117150. DOI: https://doi.org/10.1016/j.ces.2021.117150.

(37) Andreeva, I. V.; Zaitsau, D. H.; Qian, S.; Turovtzev, V. V.; Pimerzin, A. A.; Bara, J. E.; Verevkin, S. P. Glycerol valorisation towards biofuel additivities: Thermodynamic studies of glycerol ethers. *Chemical Engineering Science* **2022**, *247*, 117032. DOI: https://doi.org/10.1016/j.ces.2021.117032.

(38) García, J. I.; García-Marín, H.; Pires, E. Glycerol based solvents: synthesis, properties and applications. *Green Chemistry* **2014**, *16* (3), 1007-1033, 10.1039/C3GC41857J. DOI: 10.1039/C3GC41857J.

(39) Leal-Duaso, A.; Pérez, P.; Mayoral, J. A.; García, J. I.; Pires, E. Glycerol-Derived Solvents: Synthesis and Properties of Symmetric Glyceryl Diethers. *ACS Sustainable Chemistry & Engineering* **2019**, *7* (15), 13004-13014. DOI: 10.1021/acssuschemeng.9b02105.

(40) Andreeva, I. V.; Turovtsev, V. V.; Qian, S.; Bara, J. E.; Verevkin, S. P. Biofuel Additives: Thermodynamic Studies of Glycerol Ethers. *Industrial & Engineering Chemistry Research* **2022**, 61, 15407-15413. DOI: 10.1021/acs.iecr.2c02351.

(41) Flowers, B. S.; Mittenthal, M. S.; Jenkins, A. H.; Wallace, D. A.; Whitley, J. W.; Dennis, G. P.; Wang, M.; Turner, C. H.; Emel'yanenko, V. N.; Verevkin, S. P.; et al. 1,2,3-Trimethoxypropane: A Glycerol-Derived Physical Solvent for CO2 Absorption. *ACS Sustainable Chemistry & Engineering* **2017**, *5* (1), 911-921. DOI: 10.1021/acssuschemeng.6b02231.

(42) Sutter, M.; Pehlivan, L.; Lafon, R.; Dayoub, W.; Raoul, Y.; Métay, E.; Lemaire, M. 1,2,3-Trimethoxypropane, a glycerol-based solvent with low toxicity: new utilization for the reduction of nitrile, nitro, ester, and acid functional groups with TMDS and a metal catalyst. *Green Chemistry* **2013**, *15* (11), 3020-3026, 10.1039/C3GC41082J. DOI: 10.1039/C3GC41082J.

(43) Weininger, D. SMILES, a chemical language and information system. 1. Introduction to methodology and encoding rules. *Journal of Chemical Information and Computer Sciences* **1988**, *28* (1), 31-36. DOI: 10.1021/ci00057a005.

(44) O'Boyle, N. M.; Banck, M.; James, C. A.; Morley, C.; Vandermeersch, T.; Hutchison, G. R. Open Babel: An open chemical toolbox. *Journal of Cheminformatics* **2011**, *3* (1), 33. DOI: 10.1186/1758-2946-3-33.

(45) Spicher, S.; Grimme, S. Robust Atomistic Modeling of Materials, Organometallic, and Biochemical Systems. *Angewandte Chemie International Edition* **2020**, *59* (36), 15665-15673. DOI: https://doi.org/10.1002/anie.202004239.

(46) Grimme, S. Exploration of Chemical Compound, Conformer, and Reaction Space with Meta-Dynamics Simulations Based on Tight-Binding Quantum Chemical Calculations. *Journal of Chemical Theory and Computation* **2019**, *15* (5), 2847-2862. DOI: 10.1021/acs.jctc.9b00143.

(47) *Semiempirical extended tight-binding program xtb*; https://github.com/grimme-lab/xtb (accessed February, 2021).

(48) Bannwarth, C.; Ehlert, S.; Grimme, S. GFN2-xTB—An Accurate and Broadly Parametrized Self-Consistent Tight-Binding Quantum Chemical Method with Multipole Electrostatics and Density-Dependent Dispersion Contributions. *Journal of Chemical Theory and Computation* **2019**, *15* (3), 1652-1671. DOI: 10.1021/acs.jctc.8b01176.

(49) Soyemi, A.; Szilvási, T. Benchmarking Semiempirical QM Methods for Calculating the Dipole Moment of Organic Molecules. *The Journal of Physical Chemistry A* **2022**, *126* (11), 1905-1921. DOI: 10.1021/acs.jpca.1c10144.

(50) *Gaussian 16 Rev. C.01*; Wallingford, CT, 2016.

(51) Becke, A. D. Density-functional thermochemistry. III. The role of exact exchange. *The Journal of Chemical Physics* **1993**, *98* (7), 5648-5652. DOI: 10.1063/1.464913.

(52) Grimme, S.; Ehrlich, S.; Goerigk, L. Effect of the damping function in dispersion corrected density functional theory. *Journal of Computational Chemistry* **2011**, *32* (7), 1456-1465. DOI: https://doi.org/10.1002/jcc.21759.

(53) Weigend, F.; Ahlrichs, R. Balanced basis sets of split valence, triple zeta valence and quadruple zeta valence quality for H to Rn: Design and assessment of accuracy. *physical chemistry chemical physics* **2005**, *7* (18), 3297-3305. DOI: 10.1039/B508541A.

(54) *BIOVIA COSMOtherm*; Dassault Systèmes: http://www.3ds.com (accessed 2022/07/01)..

(55) Perdew, J. P. Density-functional approximation for the correlation energy of the inhomogeneous electron gas. *Physical Review B* **1986**, *33* (12), 8822-8824. DOI: 10.1103/PhysRevB.33.8822.

(56) Becke, A. D. Density-functional exchange-energy approximation with correct asymptotic behavior. *Physical Review A* **1988**, *38* (6), 3098-3100. DOI: 10.1103/PhysRevA.38.3098.

(57) Schäfer, A.; Huber, C.; Ahlrichs, R. Fully optimized contracted Gaussian basis sets of triple zeta valence quality for atoms Li to Kr. *The Journal of Chemical Physics* **1994**, *100* (8), 5829-5835. DOI: 10.1063/1.467146 (acccessed 2021/05/22).

(58) Eckert, F.; Klamt, A. Fast solvent screening via quantum chemistry: COSMO-RS approach. *AIChE Journal* **2002**, *48* (2), 369-385, https://doi.org/10.1002/aic.690480220. DOI: https://doi.org/10.1002/aic.690480220 (acccessed 2021/05/22).

(59) Klamt, A.; Eckert, F. COSMO-RS: a novel and efficient method for the a priori prediction of thermophysical data of liquids. *Fluid Phase Equilibria* **2000**, *172* (1), 43-72. DOI: 10.1016/S0378-3812(00)00357-5.

(60) Qian, S.; Mileski, P.; Irvin, A. C.; Soyemi, A.; Szilvási, T.; Bara, J. E. Experimental and Computational Study of the Properties of Imidazole Compounds with Branched and Cycloalkyl Substituents. In *Liquids*, 2022; Vol. 2, pp 14-25.

(61) Klamt, A.; Eckert, F.; Arlt, W. COSMO-RS: An Alternative to Simulation for Calculating Thermodynamic Properties of Liquid Mixtures. *Annual Review of Chemical and Biomolecular Engineering* **2010**, *1* (1), 101-122. DOI: 10.1146/annurev-chembioeng-073009-100903 (acccessed 2021/11/10).

(62) Lahtela, V.; Hyvärinen, M.; Kärki, T. Composition of Plastic Fractions in Waste Streams: Toward More Efficient Recycling and Utilization. *Polymers*, **2019**, 11 (1), 69. DOI: https://doi.org/10.3390/polym11010069 .

(63) Hansen, C. M. *Hansen Solubility Parameters: A User's Handbook*; CRC Press, Boca Raton FL, USA. 2007.

(64) Abbott, S. H., C.M; Yamamoto, H. *Hansen Solubility Parameters in Practice - Complete with software, data, and examples*, 2nd ed.; www.hansen-solubility.com, 2009 (accessed 2022/05/2).

(65) Hansen, C. M. The three dimensional solubility parameter - key to paint component affinities: I. Solvents, plasticizers, polymers, and resins. 1967.

(66) Hou, T. J.; Xia, K.; Zhang, W.; Xu, X. J. ADME evaluation in drug discovery. 4. Prediction of aqueous solubility based on atom contribution approach. *J Chem Inf Comput Sci* **2004**, *44* (1), 266-275. DOI: 10.1021/ci034184n. From NLM.

(67) Sorkun, M. C.; Khetan, A.; Er, S. AqSolDB, a curated reference set of aqueous solubility and 2D descriptors for a diverse set of compounds. *Scientific Data* **2019**, *6* (1), 143. DOI: 10.1038/s41597-019-0151-1.

(68) Zang, Q.; Mansouri, K.; Williams, A. J.; Judson, R. S.; Allen, D. G.; Casey, W. M.; Kleinstreuer, N. C. In Silico Prediction of Physicochemical Properties of Environmental Chemicals Using Molecular Fingerprints and Machine Learning. *Journal of Chemical Information and Modeling* **2017**, *57* (1), 36-49. DOI: 10.1021/acs.jcim.6b00625.

(69) Alshehri, A. S.; Tula, A. K.; You, F.; Gani, R. Next generation pure component property estimation models: With and without machine learning techniques. *AIChE Journal* **2022**, *68* (6), e17469, https://doi.org/10.1002/aic.17469. DOI: https://doi.org/10.1002/aic.17469 (acccessed 2022/09/28).

(70) Goodfellow, I.; Bengio, Y.; Courville, A. *Deep learning*; MIT press, Cambrigde MA, USA, 2016.

(71) Pedregosa, F.; Varoquaux, G.; Gramfort, A.; Michel, V.; Thirion, B.; Grisel, O.; Blondel, M.; Prettenhofer, P.; Weiss, R.; Dubourg, V. Scikit-learn: Machine learning in Python. *the Journal of machine Learning research* **2011**, *12*, 2825-2830.

(72) Jolliffe, I. Principal Component Analysis. In *Encyclopedia of Statistics in Behavioral Science*, Wiley, New York, USA, 2005.

(73) Ruder, S. An overview of gradient descent optimization algorithms. *ArXiv* **2016**, September 15, 2016, DOI: https://doi.org/10.48550/arXiv.1609.04747 (accessed 2022/10/13).

(74) Martín Abadi, A. A., Paul Barham, Eugene Brevdo,; Zhifeng Chen, C. C., Greg S. Corrado, Andy Davis,; Jeffrey Dean, M. D., Sanjay Ghemawat, Ian Goodfellow,; Andrew Harp, G. I., Michael Isard, Rafal Jozefowicz, Yangqing Jia,; Lukasz Kaiser, M. K., Josh Levenberg, Dan Mané, Mike Schuster,; Rajat Monga, S. M., Derek Murray, Chris Olah, Jonathon Shlens,; Benoit

Steiner, I. S., Kunal Talwar, Paul Tucker,; Vincent Vanhoucke, V. V., Fernanda Viégas,; Oriol Vinyals, P. W., Martin Wattenberg, Martin Wicke,; Yuan Yu, a. X. Z. TensorFlow: Large-scale machine learning on heterogeneous systems. In *12th USENIX Symposium on Operating Systems Design and Implementation*, Savannah, GA, USA, 2016.

(75) *Google. Welcome to Colaboratory!.* https://colab.research.google.com/gist/lzhou1110/2a30a81cb8c175514ed627bc18016774/hello-colaboratory.ipynb (accessed 2022/08/10).

(76) Prasad, S.; Brooks, B. R. A deep learning approach for the blind logP prediction in SAMPL6 challenge. *Journal of Computer-Aided Molecular Design* **2020**, *34* (5), 535-542. DOI: 10.1007/s10822-020-00292-3.

(77) Ma, J.; Sheridan, R. P.; Liaw, A.; Dahl, G. E.; Svetnik, V. Deep Neural Nets as a Method for Quantitative Structure–Activity Relationships. *Journal of Chemical Information and Modeling* **2015**, *55* (2), 263-274. DOI: 10.1021/ci500747n.

(78) Ghasemi, F.; Mehridehnavi, A.; Fassihi, A.; Pérez-Sánchez, H. Deep neural network in QSAR studies using deep belief network. *Applied Soft Computing* **2018**, *62*, 251-258. DOI: https://doi.org/10.1016/j.asoc.2017.09.040.

(79) Lusci, A.; Pollastri, G.; Baldi, P. Deep Architectures and Deep Learning in Chemoinformatics: The Prediction of Aqueous Solubility for Drug-Like Molecules. *Journal of Chemical Information and Modeling* **2013**, *53* (7), 1563-1575. DOI: 10.1021/ci400187y.

(80) Agarap, A. F. Deep Learning using Rectified Linear Units (ReLU). *ArXiv* **2018**, March 22, 2018, DOI:

https://doi.org/10.48550/arXiv.1803.08375 *(accessed 2022/10/13)*.

(81) Srivastava, N.; Hinton, G.; Krizhevsky, A.; Sutskever, I.; Salakhutdinov, R. Dropout: a simple way to prevent neural networks from overfitting. *The journal of machine learning research* **2014**, *15* (1), 1929-1958.

(82) Xu, B.; Wang, N.; Chen, T.; Li, M. Empirical Evaluation of Rectified Activations in Convolutional Network. *ArXiv* **2015**, May 5, 2015, DOI: https://doi.org/10.48550/arXiv.1505.00853 *(accessed 2022/10/13)*.

(83) Yang, K.; Swanson, K.; Jin, W.; Coley, C.; Eiden, P.; Gao, H.; Guzman-Perez, A.; Hopper, T.; Kelley, B.; Mathea, M.; et al. Analyzing Learned Molecular Representations for Property Prediction. *Journal of Chemical Information and Modeling* **2019**, *59* (8), 3370-3388. DOI: 10.1021/acs.jcim.9b00237.

(84) Chen, L.-Y.; Hsu, T.-W.; Hsiung, T.-C.; Li, Y.-P. Deep Learning-Based Increment Theory for Formation Enthalpy Predictions. *The Journal of Physical Chemistry A* **2022**, *126* (41), 7548-7556. DOI: 10.1021/acs.jpca.2c04848.

(85) Li, L.; Lu, Z.; Liu, G.; Tang, Y.; Li, W. In Silico Prediction of Human and Rat Liver Microsomal Stability via Machine Learning Methods. *Chemical Research in Toxicology* **2022**, *35* (9), 1614-1624. DOI: 10.1021/acs.chemrestox.2c00207.

(86) Yang, K.; Swanson, K.; Jin, W.; Coley, C.; Eiden, P.; Gao, H.; Guzman-Perez, A.; Hopper, T.; Kelley, B.; Mathea, M.; et al. Analyzing Learned Molecular Representations for Property Prediction. *Journal of Chemical Information and Modeling* **2019**, *59* (8), 3370-3388. DOI: 10.1021/acs.jcim.9b00237.

(87) *Molecular Property Prediction* https://github.com/chemprop/chemprop (accessed November 17, 2022).

(88) Bradley, J.-C.; Lang, A.; Williams, A. Jean-Claude Bradley double plus good (highly curated and validated) melting point dataset. *Figshare* **2014**, *10*, m9, DOI: http://dx.doi.org/10.6084/m9.figshare.1031637.

(89) Tetko, I. V.; M. Lowe, D.; Williams, A. J. The development of models to predict melting and pyrolysis point data associated with several hundred thousand compounds mined from PATENTS. *Journal of Cheminformatics* **2016**, *8* (1), 2. DOI: 10.1186/s13321-016-0113-y.

(90) Morgan, H. L. The Generation of a Unique Machine Description for Chemical Structures-A Technique Developed at Chemical Abstracts Service. *Journal of Chemical Documentation* **1965**, *5* (2), 107-113. DOI: 10.1021/c160017a018.

(91) Moldoveanu, S. C.; David., V. Intermolecular Interactions. In *Essentials in Modern HPLC Separations*, 2nd ed. Elsevier, 2013, pp 147-176

(92) Leal-Duaso, A.; Pérez, P.; Mayoral, J. A.; Pires, E.; García, J. I. Glycerol as a source of designer solvents: physicochemical properties of low melting mixtures containing glycerol ethers and ammonium salts. *Physical Chemistry Chemical Physics* **2017**, *19* (41), 28302-28312, 10.1039/C7CP04987K. DOI: 10.1039/C7CP04987K.

(93) Petrucci, R. H., F. Geoffrey Herring, Jeffrey D. Madura, Carey Bissonnette. *General Chemistry: Principles and Modern Applications*; Pearson Education, New York, USA, 2011.

(94) Wang, K.; Jirka, M.; Rai, P.; Twieg, R. J.; Szilvási, T.; Yu, H.; Abbott, N. L.; Mavrikakis, M. Synthesis and properties of hydroxy tail-terminated cyanobiphenyl liquid crystals. *Liquid Crystals* **2019**, *46* (3), 397-407. DOI: 10.1080/02678292.2018.1502373.

(95) Wang, K.; Szilvási, T.; Gold, J.; Yu, H.; Bao, N.; Rai, P.; Mavrikakis, M.; Abbott, N. L.; Twieg, R. J. New room temperature nematogens by cyano tail termination of alkoxy and alkylcyanobiphenyls and their anchoring behavior on metal salt-decorated surface. *Liquid Crystals* **2020**, *47* (4), 540-556. DOI: 10.1080/02678292.2019.1662116.

(96) Wang, K.; Rahman, M. S.; Szilvási, T.; Gold, J. I.; Bao, N.; Yu, H.; Abbott, N. L.; Mavrikakis, M.; Twieg, R. J. Influence of multifluorophenyloxy terminus on the mesomorphism of the alkoxy and alkyl cyanobiphenyl compounds in search of new ambient nematic liquid crystals and mixtures. *Liquid Crystals* **2021**, *48* (5), 672-688. DOI: 10.1080/02678292.2020.1810792.

(97) Wang, K.; Rai, P.; Fernando, A.; Szilvási, T.; Yu, H.; Abbott, N. L.; Mavrikakis, M.; Twieg, R. J. Synthesis and properties of fluorine tail-terminated cyanobiphenyls and terphenyls for chemoresponsive liquid crystals. *Liquid Crystals* **2020**, *47* (1), 3-16. DOI: 10.1080/02678292.2019.1616228.

(98) Hermens, J. L. M.; de Bruijn, J. H. M.; Brooke, D. N. The octanol–water partition coefficient: Strengths and limitations. *Environmental Toxicology and Chemistry* **2013**, *32* (4), 732-733, https://doi.org/10.1002/etc.2141. DOI: https://doi.org/10.1002/etc.2141 (acccessed 2023/02/07).

(99) Min, K.; Cuiffi, J. D.; Mathers, R. T. Ranking environmental degradation trends of plastic marine debris based on physical properties and molecular structure. *Nature Communications* **2020**, *11* (1), 727. DOI: 10.1038/s41467-020-14538-z.

(100) Cavallo, G.; Metrangolo, P.; Milani, R.; Pilati, T.; Priimagi, A.; Resnati, G.; Terraneo, G. The Halogen Bond. *Chemical Reviews* **2016**, *116* (4), 2478-2601. DOI: 10.1021/acs.chemrev.5b00484.

(101) Müller, K. 2 - Fluorination patterns in small alkyl groups: their impact on properties relevant to drug discovery. In *Fluorine in Life Sciences: Pharmaceuticals, Medicinal Diagnostics, and Agrochemicals*, Haufe, G., Leroux, F. R. Eds.; Academic Press, Cambridge MA, USA, 2019; pp 91-139.

(102) Copley, M. J.; Ginsberg, E.; Zellhoefer, G. F.; Marvel, C. S. Hydrogen Bonding and the Solubility of Alcohols and Amines in Organic Solvents. XIII. *Journal of the American Chemical Society* **1941**, *63* (1), 254-256. DOI: 10.1021/ja01846a059.

(103) Stephenson, R. M. Mutual solubility of water and aliphatic amines. *Journal of Chemical & Engineering Data* **1993**, *38* (4), 625-629. DOI: 10.1021/je00012a039.

(104) Petcore. *Post consumer PET recycling in Europe*; 2010. (accessed 10/21/2022).

(105) Venkatram, S.; Kim, C.; Chandrasekaran, A.; Ramprasad, R. Critical Assessment of the Hildebrand and Hansen Solubility Parameters for Polymers. *Journal of Chemical Information and Modeling* **2019**, *59* (10), 4188-4194. DOI: 10.1021/acs.jcim.9b00656.

(106) Miller-Chou, B. A.; Koenig, J. L. A review of polymer dissolution. *Progress in Polymer Science* **2003**, *28* (8), 1223-1270. DOI: https://doi.org/10.1016/S0079-6700(03)00045-5.

TOC:

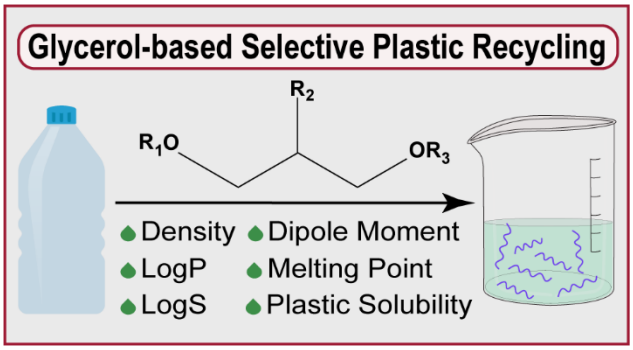
Glycerol-based Selective Plastic Recycling
R2
R1O
OR3
Density
Dipole Moment
LogP
Melting Point
LogS
Plastic Solubility